



# A combination of inhibiting microglia activity and remodeling gut microenvironment suppresses the development and progression of experimental autoimmune uveitis



Jianhong Zhou<sup>a,b</sup>, Jingjing Yang<sup>a,b</sup>, Mali Dai<sup>a,b</sup>, Dan Lin<sup>a,b</sup>, Renshu Zhang<sup>a,b</sup>, Hui Liu<sup>a,b</sup>, Ailing Yu<sup>a,b</sup>, Serhii Vakal<sup>c</sup>, Yuqin Wang<sup>a,b,\*</sup>, Xingyi Li<sup>a,b,\*</sup>

<sup>a</sup> School of Ophthalmology & Optometry and Eye Hospital, Institute of Biomedical Engineering, Wenzhou Medical University, Wenzhou 325027, Zhejiang, China

<sup>b</sup> State Key Laboratory of Optometry & Vision Science, Wenzhou 325027, Zhejiang, China

<sup>c</sup> Structural Bioinformatics Laboratory, Biochemistry, Åbo Akademi University, Turku 20541, Finland

## ARTICLE INFO

### Keywords:

Experimental autoimmune uveitis (EAU)

Minocycline

Microglial activation

Gut microbiota

Metabolism

## ABSTRACT

Noninfectious (autoimmune and immune-mediated) uveitis is an ocular inflammatory disease which can lead to blindness in severe cases. Due to the potential side effects of first-line drugs for clinical uveitis, novel drugs and targets against uveitis are still urgently needed. In the present study, using rat experimental autoimmune uveitis (EAU) model, we first found that minocycline treatment can substantially inhibit the development of EAU and improve the retinal function by suppressing the retinal microglial activation, and block the infiltration of inflammatory cells, including Th17, into the retina by decreasing the major histocompatibility complex class II (MHC II) expression in resident and infiltrating cells. Moreover, we demonstrated that minocycline treatment can remodel the gut microenvironment of EAU rats by restoring the relative abundance of *Ruminococcus bromii*, *Streptococcus hyoilealis*, and *Desulfovibrio* sp. ABHU2SB and promoting a functional shift in the gut via reversing the levels of L-proline, allixin, aceturic acid, xanthine, and leukotriene B4, and especially increasing the production of propionic acid, histamine, and pantothenic acid. At last, we revealed that minocycline treatment can significantly attenuate the progression of EAU after inflammation onset, which may be explained by the role of minocycline in the remodeling of the gut microenvironment since selective elimination of retinal microglia on the later stages of EAU was shown to have little effect. These data clearly demonstrated that inhibition of microglial activation and remodeling of the gut microenvironment can suppress the development and progression of experimental autoimmune uveitis. Considering the excellent safety profile of minocycline in multiple clinical experiments, we suggest that minocycline may have therapeutic implications for clinical uveitis.

## 1. Introduction

Noninfectious (autoimmune and immune-mediated) uveitis is a sight-threatening, even blindness-causing ocular inflammatory disease that is responsible for 5–20% cases of blindness in the developed and developing countries [1,2]. Clinically, noninfectious uveitis can be found in birdshot retinochoroidopathy, sympathetic ophthalmia, idiopathic uveitis, and many systemic autoimmune diseases such as Behcet's disease, sarcoidosis, and Vogt-Koyanagi-Harada disease. Due to its pathogenic complexity, uveitis has become a serious public concern [3,4]. Experimental autoimmune uveitis (EAU), an established animal model resembling human autoimmune uveitis, is widely used to delineate the immunopathogenesis of autoimmune uveitis. Through this

animal model, the genetic and environmental factors were shown to be the main reasons for triggering the noninfectious uveitis, among which the CD4 positive T-cell subsets-mediated immune imbalance, especially the Th1 and Th17 responses, was proven to play a critical role in the initiation and progression of the disease. However, up to now, immunosuppressive agents such as cyclosporin A and corticosteroids have been the first-line clinical drugs for human uveitis, and, due to their potential side effects, the novel targets and treatments with high safety and efficiency profiles are still strongly needed.

Last decades, following the explosion of research into the underlying pathogenesis of EAU, the crucial roles of retinal microglia and gut commensal microbes have drawn more and more attention from researchers. Retinal microglia, as resident immune cells mainly located in

\* Corresponding authors at: School of Ophthalmology & Optometry and Eye Hospital, Wenzhou Medical University, 270 Xueyuan Road, Wenzhou 325027, Zhejiang, China.

E-mail addresses: [wangyuqin@mail.eye.ac.cn](mailto:wangyuqin@mail.eye.ac.cn) (Y. Wang), [lixingyi\\_1984@mail.eye.ac.cn](mailto:lixingyi_1984@mail.eye.ac.cn) (X. Li).

the inner retina, are abnormally activated in a variety of retinal diseases, including pathological retinal angiogenesis [5], retinal detachment [6], retinal degeneration [7], diabetic retinopathy [8], and autoimmune uveitis [9,10]. More importantly, Okunuki et al. recently showed that local deletion of the retinal microglia can significantly suppress the onset of EAU, which means that decreasing the microglial activation may inhibit the EAU [11]. Additionally, the dysfunction of gut microbiota has been found in many inflammatory autoimmune diseases, such as inflammatory bowel disease (IBD) [12,13], systemic lupus erythematosus (SLE) [14], rheumatoid arthritis (RA) [15], multiple sclerosis (MS) [16,17], Behcet's disease (BD) [18] and Vogt-Koyanagi-Harada disease (VKHD) [19]. Although the causative relationship between the gut microbiota and uveitis is not well-established yet, the critical roles of gut microbiota in modulating the initiation and progression of uveitis in human and animals cannot be ignored, since the removal of gut microbiota can significantly attenuate the EAU [20,21], the surrogate antigen from gut microbiota can trigger autoimmunity in an immune-privileged site [22], and fecal microbiota transplantation from BD and VKHD patients can significantly exacerbate EAU disease in the recipient mice [18,19]. This evidence suggests that abnormal microglial activities and dysfunction of gut microbiome play vital roles in the onset and progression of EAU.

Considering the above-mentioned, the pleiotropic effects of minocycline aroused our intensive interest. Minocycline (MINO) is a blood-brain/retina barrier permeable semisynthetic tetracycline with well-known antimicrobial and microglia-inactivating effects. In addition to impressive neuroprotection against various central nervous system diseases via anti-neuroinflammation, anti-apoptosis, immunomodulation, and inhibition of microglia activation [23], minocycline has also been proven to confer promising protection against multiple retinal diseases such as diabetic retinopathy [24], retinal degeneration [7,25,26], retinal ischemia [27,28], branch retinal vein occlusion [29] and glaucoma [30]. As a broad-spectrum antibiotic, minocycline can also affect the gut microbiome, which also has been proven to play a critical role in its anti-depression function [31,32]. More importantly, several clinical trials have revealed that minocycline treatment can ameliorate various neurological diseases, including cognitive deficits, depression, and fragile X syndrome [33,34] with excellent safety and tolerance profiles. However, until now, the effects of minocycline on the non-infection uveitis, especially the underlying mechanism, remain unknown. Thus, in this study, we adopt rat experimental autoimmune uveitis (EAU) with optical coherence tomography (OCT), electroretinography (ERG), immunohistochemistry (IHC) and analysis of gut microbiome and metabolism to systematically explore the effects of minocycline in the non-infection uveitis and the possible underlying mechanisms, and eventually provide reliable data to support the clinical introduction of minocycline as a treatment for clinical uveitis.

## 2. Materials and methods

### 2.1. Experimental autoimmune uveitis

Lewis male rats (about 180 g) were obtained from Beijing Vital River Laboratory Animal Technology Co., Ltd. EAU was induced according to our previous protocol with minor modifications [35]. Briefly, 2.5 mg hIRBP161–180 (Shanghai Sangon Biological Engineering Technology & Services Co., Ltd.) in 2.5 ml PBS solution was firstly emulsified with a complete Freund's adjuvant containing 2.5 mg/ml Mycobacterium Tuberculosis H37Ra (Difco Laboratories, Detroit, MI) (1:1; v/v) and then subcutaneously injected into the left hind footpads of the Lewis rats (100 µl per rat). The day of immunization was identified as Day 0 (D0). All the animal experiments were carried out following the approved guidelines of the Wenzhou Medical University Institutional Animal Care and Use Committee.

### 2.2. Clinical and histological assessment of EAU

Clinical scores were evaluated every other day by an experienced ophthalmologist starting from D6 after immunization with a slit-lamp biomicroscope (SLM-8E, Chongqing Kang Huarui Ming Technology co., LTD) until the end of the experiment, and the standard of the clinical score was as follows [41]: 0 = no disease; 1 = mild iridocyclitis with abnormal pupil configuration; 2 = moderate iridocyclitis with synechia and empyema; 3 = severe iridocyclitis with massive empyema; 4 = panophthalmitis with bleeding and corneal neovascularization.

At the end of the experiment, the entire eyeballs of the euthanized animals were freshly harvested, fixed, sliced, and stained with hematoxylin and eosin (H&E, Beyotime Biotechnology, China) for histopathological evaluation. The histopathological assessment for sections was based on the amounts of infiltrating inflammatory cell on a scale of 0–4 [41]: 0 = healthy retinal structure, no inflammatory cell infiltration; 1 = mild inflammatory cell infiltration of the retina; 2 = moderate inflammatory cell infiltration of the retina and the damage of outer nuclear layer; 3 = excessive inflammatory cell infiltration of the retina involving the damage of internal limiting membrane, and 4 = excessive inflammatory cell infiltration of the retina with full-thickness retinal damage.

### 2.3. Minocycline treatment

Minocycline (Shanghai Haling Biotechnology Co., Ltd, China) was prepared freshly in phosphate buffer saline (PBS) as described previously [7]. All the EAU rats were randomly divided into minocycline-treated EAU groups (MINO + EAU) and PBS-treated EAU groups and respectively treated with minocycline (25 mg/kg or 50 mg/kg) or vehicle PBS in the same volume by intraperitoneal injection (i.p.). The non-immunized rats were considered as control groups injected with the same volume of PBS. Two different treatment periods (D0-D14 or D8-D18) were implemented to investigate the effect of minocycline on the initiation and progression of EAU, respectively.

### 2.4. Immunohistochemistry

After eyeballs were collected, isolated and fixed, the retinas were sliced into 10-µm-thick cryosections. First, all the sections were blocked and permeabilized with blocking solution (0.3% Triton X-100, 0.2% BSA, and 5% goat serum in PBS, Beyotime Biotechnology, China), then incubated with the following primary antibodies: IBA1 (Wako, 019-19741), CD68 (Bio-Rad, MCA341GA), IL-1 $\beta$  (R&D Systems, AF-401-SP), GFAP (Abcam, ab7260), CD4 (Invitrogen, MA1-81588; Invitrogen, 14-0041-82), CD45 (BD Pharmingen, 550566), IL-17 (Santa Cruz, SC-374218), P2ry12 (Anaspec, AS-55043A) and MHC class II (Invitrogen, 14-5321-82). All the primary antibodies were incubated at least for 24 h at 4 °C. After three 5-min rinses with PBS, fluorescence-conjugated secondary antibodies (1:500; Invitrogen, Life Technologies) were applied to detect the positive signal. Finally, DAPI dye was used to stain the cell nuclei. The mean fluorescence values were obtained by Image J software.

### 2.5. Terminal deoxynucleotidyl transferase biotin-dUTP nick end labeling (TUNEL) assay

TUNEL staining (*In Situ* Cell Death Detection kit) was used to evaluate the rat retinal cell apoptosis at D14 according to the manufacturer's instructions (Roche Diagnostics, Basel, Switzerland). After permeabilization, antigen retrieval was performed in 10-µm-thick cryostat sections by 0.1% sodium citrate buffer solution containing 0.5% Triton X-100 for 5 min. After three 8-min washes, all the sections were treated with TUNEL reaction solutions for 1 h at 37 °C, then counterstained with DAPI (1:2500; Beyotime Biotechnology, China). TUNEL-positive cells from sections were evaluated under fluorescence

microscopy (Zeiss 510; Carl Zeiss AG, Germany).

#### 2.6. High-resolution spectral-domain optical coherence tomography imaging

The rats were systemically anesthetized, and the pupils were dilated with 0.5% tropicamide (Santen Pharmaceutical Co., Ltd, Japan). Optical coherence tomography (OCT) images were acquired using a high-resolution spectral-domain optical coherence tomography (SD-OCT) imaging instrument (Micron IV, Phoenix Research Laboratories, USA) on D14 after immunization by an experienced ophthalmologist. Each final SD-OCT image was constructed from 80 pictures. The assessment of retinal inflammation was implemented using a double-blind approach.

#### 2.7. Labeling of adherent leukocytes in retinal vessels

To analyze the effect of minocycline on adherent retinal leukocytes, FITC-Concanavalin A lectin (FITC-ConA, C7642, Sigma) was used to visualize the retinal vasculature and adherent leukocytes according to Van Hove et al., with minor modifications [36]. Briefly, after deep anesthesia, rats were first transcardially perfused with 30 ml of PBS to remove the blood and non-adherent leukocytes, then perfused with 25 ml of FITC-ConA (40 µg/ml in PBS 1X, pH 7.5) to stain adherent leukocytes and vascular endothelial cells. At last, an additional 30 ml of PBS were injected to remove the unbound FITC-ConA. After that, the eyes were immediately isolated and stored in 4% paraformaldehyde in 0.1 M PBS for 20 min. After the retinas were dissected and flat-mounted, the total number of FITC-ConA-stained adherent leukocytes was counted with a fluorescent microscope (Axio Observer Z1; Carl Zeiss).

#### 2.8. Electoretinographic analysis

Electoretinographic responses from control, EAU, and Mino-EAU groups were recorded with a custom-built Ganzfeld dome system (Roland Q400, Wiesbaden, Germany) on D12 post-immunization [37]. After dark adaptation overnight, the rats were anesthetized intraperitoneally with 10% chloral hydrate (Beyotime Biotechnology, China). Atropine sulfate (Shenyang Xingqi Pharmaceutical Co., Ltd, China) and proparacaine hydrochloride (Alcon Ophthalmic Product Co., Ltd, China) were used to, respectively, dilate the pupils and anesthetize the corneas. For recording, custom golden-ring electrodes were placed at the center of the cornea, and the reference and ground electrodes were separately inserted into the cheek and tail. To maximize retinal sensitivity, the whole recording processes were conducted under dim red light. Scotopic, rod-mediated responses were obtained from dark-adapted animals at 3 cd.s/m<sup>2</sup> light intensities. Photopic, cone-mediated responses were performed following 10-min light adaptation and recorded at the light intensity of 5 cd.s/m<sup>2</sup>. At least five rats per each group were recorded.

#### 2.9. Evans blue staining

To examine the role of minocycline in the integrity and permeability of the blood-retina barrier (BRB), Evans blue dye was used as described previously [38]. In brief, 400 µl of 2% (wt/vol) Evans blue (Sigma-Aldrich, USA) was injected into the tail veins. Two hours later, the eyes were enucleated and immediately fixed in 4% paraformaldehyde (Beyotime Biotechnology, China) for another 2 h. After removing the anterior segments, the retinas were dissected and washed in cold PBS for 20 min. Finally, the retinas were flat-mounted with the vitreous side facing up. All the pictures were taken under a fluorescent microscope.

#### 2.10. 16S rRNA microbiota analysis

The fresh cecal contents were harvested and stored at -80 °C. The

total DNA was extracted using a TIANamp Stool DNA kit (TIANGEN Bio-Tech Co., Ltd, Beijing, China) according to the manufacturer's protocol. The V3-V4 hypervariable region of the bacterial 16S ribosomal RNA gene was amplified as previously reported [39]. 16S rRNA amplicons were sequenced with the Illumina HiSeq platform according to standard protocols. The bioinformatics analyses were also carried out according to previous studies [40]. Briefly, after the effective tags were obtained by QIIME 1.7.0 quality control process and UCHIME algorithm-based comparison and detection [41,42], the same operational taxonomic units (OTUs) with 97% sequence similarity were classified by UPARSE software and multiple sequence alignments were performed using MUSCLE software [43,44]. Alpha diversity and beta diversity were calculated with QIIME (Version 1.7.0) and visualized with R software (Version 2.15.3). LDA effect size (LefSe) was used to detect the difference of the dominant bacterial community between groups.

#### 2.11. Untargeted metabolomics study

The approaches of untargeted metabolomics in this work were applied according to the paper by Sun et al. (2019) but with minor modifications [39]. After the harvested feces (200 mg) were grounded, resuspended, centrifuged, and filtered, the collected filtrate was injected into the LC-MS/MS system using a Vanquish UHPLC system (Thermo Fisher) coupled with an Orbitrap Q Exactive HF-X mass spectrometer (Thermo Fisher). Eluent A (5 mM ammonium acetate, pH 9.0) and eluent B (methanol, Sigma) were used as eluents for the negative polarity mode, eluent A (0.1% FA in Water) and eluent B (methanol, Sigma) were used for the positive polarity mode. The solvent gradient was: 2% methanol for 1.5 min, 2–100% methanol for 12.0 min, 100% methanol for 14.0 min, 100–2% methanol for 14.1 min and 2% methanol for 16.0 min. Q Exactive HF-X mass spectrometer was operated in the positive/negative polarity mode with a spray voltage of 3.2 kV, the capillary temperature of 320 °C, sheath gas flow rate of 35 arb, and aux gas flow rate of 10 arb. The raw data were processed using the Compound Discoverer 3.0 (Thermo Fisher Scientific) to perform peak alignment, peak picking, and quantitation of each metabolite. The principal component analysis (PCA) was performed by the SIMCA-P software package (v13.0, Umetrics, Umeå, Sweden).

#### 2.12. Quantification and statistical analysis

All data were presented as mean ± standard error of the mean (SEM). Two-way analysis of variance (ANOVA) for repeated measures with post hoc Bonferroni's test was used for the comparison of the data of clinical score. Differences between two groups were analyzed using an unpaired *t*-test. Differences among the three groups were assessed by one-way ANOVA, followed by Tukey's or Dunnett's multiple comparison test. All statistical comparisons were performed using SPSS statistics version 25. The significance of the differences was marked as follows in the figures: \* p < 0.05, \*\* p < 0.01 and \*\*\* p < 0.001.

### 3. Results

#### 3.1. Minocycline limited the pathological development of EAU both clinically and histopathologically

As expected, all the EAU rats treated with PBS gradually developed severe uveitis with dilated vessels, severe hypopyon and massive leakage of inflammatory cells on day 14 post-immunization (Fig. 1B, EAU), as revealed by slit-lamp examination, but 50 mg/kg minocycline treatment dramatically mitigated these ocular pathological symptoms (Fig. 1B, MINO + EAU, 50 mg/kg). In contrast, 25 mg/kg minocycline treatment was associated with ocular pathological symptoms similar to the EAU group (Fig. 1B, MINO + EAU, 25 mg/kg). The clinical score also indicated that 50 mg/kg minocycline treatment significantly reduced the EAU severity when compared to the PBS-treated immunized

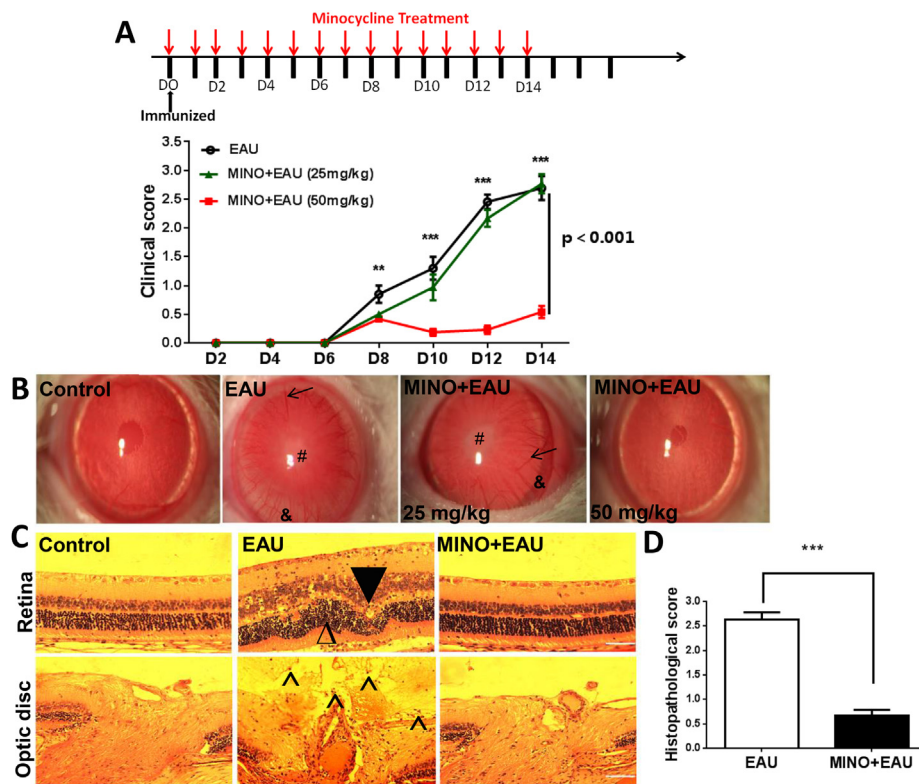


**Fig. 1.** Minocycline countered the pathological development of EAU, both clinically and histopathologically. (A) The schematic time course of minocycline treatment (top). Time course of EAU clinical scores ( $n \geq 8$  rats per group) by slit-lamp observation. EAU group treated with the same volume of PBS as minocycline treatment; MINO + EAU group (25 mg/kg) was intraperitoneally (i.p.) injected with 25 mg/kg minocycline per day starting from day 0 (D0); MINO + EAU group (50 mg/kg) was injected with 50 mg/kg minocycline per day starting from day 0 (D0); Two-way ANOVA for repeated measures with post hoc Bonferroni's test was used for the comparison of clinical score data. (B) Representative ocular images of different groups by slit-lamp observation on day 14 (D14) post-immunization. Dilated vessels (→), severe hypopyon (&) massive leakage of inflammatory cells (#) were observed in EAU and MINO + EAU (25 mg/kg) groups but absent in control and MINO + EAU (50 mg/kg) groups. (C) Representative histopathological pictures by H&E staining. Infiltration of inflammatory immune cells (\*) in the vitreous body together with photoreceptor folds (Δ) and vasculitis (▲) were observed in the EAU group but not control or MINO + EAU (50 mg/kg) groups. (D) Histopathological EAU scores on D14 ( $n \geq 5$  rats per group) were graded in a blinded manner. T-test was used to analyze histopathological scores. All the data are expressed as mean  $\pm$  SEM. \* –  $p < 0.05$ ; \*\* –  $p < 0.01$ ; \*\*\* –  $p < 0.001$ .

rats, but not 25 mg/kg minocycline treatment (Fig. 1A, two-way ANOVA for repeated measures with post hoc Bonferroni's test, the group effect between 50 mg/kg minocycline + EAU and EAU groups,  $p < 0.001$ ; the significance of the differences on D8, D10, D12 and D14 between 50 mg/kg minocycline + EAU and EAU groups, \*\*  $p < 0.01$  and \*\*\*  $p < 0.001$ ; the group effect between 50 mg/kg minocycline + EAU and 25 mg/kg minocycline + EAU groups,  $p < 0.001$ ; the group effect between 25 mg/kg minocycline + EAU and EAU groups,  $p > 0.05$ ). These results suggest that minocycline mitigates the severity of EAU in a dose-dependent manner. The histopathological assessment further supported this notion. As shown in Fig. 1C-D, the EAU treated with vehicle developed severe infiltration of inflammatory immune cells in the vitreous, photoreceptor folds and vasculitis, while 50 mg/kg minocycline treatment preserved relatively normal retinal architecture and exhibited a significant reduction of the histopathological score compared to the vehicle-treated EAU rats (Fig. 1D,  $p < 0.01$ ). All the data demonstrate that minocycline ameliorates the severity of EAU both clinically and histopathologically.

### 3.2. Minocycline treatment improved retinal function

To further assess whether minocycline treatment improves retinal function, responses of scotopic and photopic ERG were examined. We found that the retinal function was severely impaired in the immunized rats with markedly reduced response of scotopic and photopic ERG compared to the controls (Fig. 2, all  $p < 0.05$ , one-way ANOVA). Conversely, minocycline treatment well preserved the responses of scotopic ERG with regular a- and b-wave amplitudes (Fig. 2A and B,  $p < 0.05$  between EAU and MINO + EAU groups;  $p > 0.05$  between Control and MINO + EAU groups). Meanwhile, the photopic ERG b-wave amplitudes can be partially improved upon minocycline treatment when compared with immunized rats (Fig. 2C,  $p < 0.05$  between EAU and MINO + EAU groups), but still lower than the control (Fig. 2C,  $p < 0.05$  between Control and MINO + EAU groups). In summary, minocycline treatment substantially improved the impaired retinal function induced by immunization.

### 3.3. Minocycline treatment suppressed the microglial activation and downregulated retinal IL-1 $\beta$ level

Since abnormal microglial activation has been related to various retinal diseases, through retinal cryosections staining, we found that IBA1-expressing microglia were sparsely located in the inner plexiform layer of control retina (Fig. 3A, top panels), while in the immunized retina, the microglia were activated and ramified with larger cell bodies; moreover, microglia even invaded into the inner portion of the outer nuclear layer (Fig. 3A, middle panels). To label the microglial activation, CD68 (a marker for microglial activation) staining was performed, and co-staining indicated that most of microglia in the immunized retinas exerted CD68 signaling (Fig. 3A, middle panels). However, after minocycline treatment, both CD68 and IBA1 immunoreactivities were much less intensive than in the PBS-treated EAU retinas (Fig. 3A, bottom panels), and the relative quantitative analysis of IBA1 immunoreactivity showed the same results (Fig. 3C,  $p < 0.05$ , one-way ANOVA). Like what was observed with IBA1 immunoreactivity, the level of interleukin-1 beta (IL-1 $\beta$ ) released by microglia/macrophages was also significantly downregulated following minocycline treatment when compared to the EAU groups (Fig. 3B and D,  $p < 0.05$ ). While IL-1 $\beta$  is implicated in cellular apoptosis, consistently, a larger number of TUNEL-positive nuclei was detected after immunization compared to the controls. Following minocycline treatment, the number of TUNEL-positive nuclei was significantly lower when compared with PBS-treated immunized rats but still higher than the controls (Fig. 3E and F,  $p < 0.05$  between EAU and MINO + EAU groups;  $p < 0.05$  between Control and MINO + EAU groups).

### 3.4. Minocycline preserved the integrity of BRB and inhibited macrophage and Th17 infiltration of the retina

Abnormal microglial activation and increased IL-1 $\beta$  also suggested broken blood-retina barrier (BRB), so the GFAP immunoreactivity (a marker of astrocytes or activated Müller cells) was investigated by cryosection staining in this work since retinal astrocytes played an

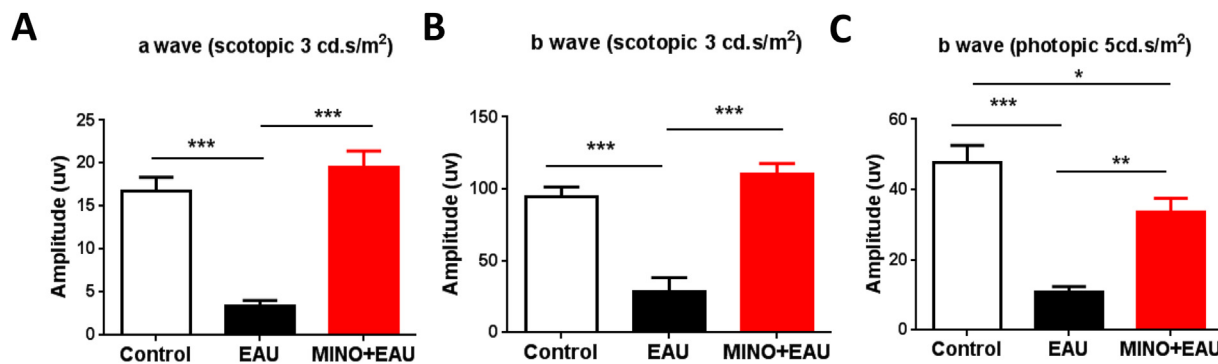


**Fig. 2.** Minocycline treatment improved retinal function. (A and B) Average scotopic a-wave (A) and b-wave (B) amplitudes elicited at 3cd.s/m<sup>2</sup> light intensities from control (white), PBS-treated (dark) and minocycline-treated (red) EAU groups. (C) Average photopic b-wave amplitude elicited at 5cd.s/m<sup>2</sup> light intensities from control (white), PBS-treated (dark), and minocycline-treated (red) groups. Values expressed as mean  $\pm$  SEM and analyzed by one-way ANOVA, followed by Tukey's multiple comparison test ( $n \geq 5$ , \* -  $p < 0.05$ ; \*\* -  $p < 0.01$ ; \*\*\* -  $p < 0.001$ ). (For interpretation of the references to color in this figure legend, the reader is referred to the web version of this article.)

essential role in maintaining the integrity of blood-retina barrier (BRB) [45]. In the control retina, the GFAP-positive astrocytes were mainly confined to the vicinity of the GCL layer (Fig. 4A, top panels). However, after immunization, the GFAP immunoreactivity was obviously elevated, and the activated Müller cells filled the whole retinal cryosections, which indicated disrupted BRB, severe gliosis, and intraocular inflammation (Fig. 4A, middle panels). Following the minocycline administration, the GFAP immunofluorescence was considerably lower compared to the PBS-treated EAU (Fig. 4A, bottom panels). Upregulated GFAP immunoreactivity suggested the disruption of BRB. In line with this pathological phenotype, the Evans blue staining demonstrated that EAU retinas were diffused with Evans blue leakage, while no apparent leakage was observed in the minocycline-treated immunized and non-immunized rats (Fig. 4B), which means that minocycline preserved the integrity and permeability of BRB. Meanwhile, the CD4 staining revealed a large number of CD4-positive cells in the PBS-treated EAU retina (Fig. 4C, CD4 immunoreactivity). Conversely, fewer T-cells were observed in retinas from the control and minocycline-treated EAU groups (Fig. 4C, CD4 immunoreactivity). Similar results can be observed by CD68 staining (Fig. 3A, CD68 immunoreactivity). This evidence revealed that minocycline can preserve the integrity of the BRB and inhibit the infiltration of macrophages and T-cells into the retina. The retinal infiltration of Th1 and Th17 cells are believed to be the main reason for triggering human and animal uveitis. Co-localization staining further showed that a more substantial amount of CD4 and IL17-positive cells resided in the immunized retina compared to the non-immunized retina (Fig. 4C). At the same time, CD4 and IL17-positive cells were barely presented in the minocycline-treated EAU groups (Fig. 4C), thus suggesting that minocycline can significantly inhibit Th17-positive cellular infiltration.

### 3.5. Minocycline reduced retinal leukocyte adhesion and vitreous leukocyte infiltration

Since deleting the retinal microglia was shown to inhibit the adhesion of retinal leukocytes and, eventually, block the recruitment of inflammatory cells to retinal vessels [11], to further explore the underlying mechanism of minocycline inhibiting Th17-positive cellular infiltration, we also examined the role of minocycline in the retinal leukocyte adhesion. As we can see from Fig. 5A, immunization caused a significant increase in the number of retinal adherent leukocytes, but minocycline treatment apparently reduced the number of adherent leukocytes when compared to EAU rats; however, the level was still higher compared to the non-immunized control rats (Fig. 5A and B). To further confirm this inhibitory effect, SD-OCT, a non-invasive *in vivo* imaging technique, was applied to quantify the number of vitreous

infiltrating leukocytes. Consistent with the retinal leukocyte adhesion, OCT pictures showed that a large number of infiltrating leukocytes were present near the optic nerve head of EAU groups, while the number in the minocycline-treated EAU and control groups was much lower (Fig. 5C). These results suggest that inhibition of microglial activities reduced the retinal leukocyte adhesion and the number of vitreous infiltrating leukocytes.

### 3.6. Minocycline decreased MHC class II expression in the retina

The resident and infiltrating cells expressing the major histocompatibility complex (MHC) class II were considered to contribute to the onset and progression of EAU as local antigen-presenting cells. To characterize the effects of minocycline on the local autoantigen presenting response, MHC class II expression was further determined by immunofluorescence staining. In naive rats, MHC class II was weakly and sparsely expressed in the inner retina, while in the immunized retina, MHC class II was globally expressed with the highest densities in the ganglion cell layer, outer plexiform layer and retinal pigment epithelium (RPE) layer (Fig. 6). Unsurprisingly, the double-labeling immunocytochemistry experiment indicated that the most MHC II-positive cells also expressed CD45 (a leukocyte marker) (Fig. 6A, middle panels), which is supported by our finding that a large number of adherent and infiltrating leukocytes is present in the EAU retinas (Fig. 5). After minocycline treatment, the immunofluorescence intensities of MHC class II and CD45 were distinctly reduced (Fig. 6A, bottom panels); the relative quantitative analysis of MHC class II is shown in Fig. 6D ( $p < 0.05$ , one-way ANOVA). Because resident cells were also capable of expressing MHC class II, to further confirm this notion, IBA1 was co-stained with MHC II. As we can see from Fig. 6B, in normal retina, IBA1-expressing cells were sparsely located in the plexiform layer, while in the immunized retina, the IBA1-positive cells were activated (with larger cell bodies and amoeboid shapes, even extended to outer nuclear layer). Co-localized images indicated that part of the IBA1-expressing cells was antigen-presenting cells (MHC II-expressing cells). Since IBA1 is a commonly used marker for macrophages and microglia, to elucidate whether local microglia can express MHC class II, P2ry12 antibody, a newly established microglia-specific marker, was used. Consistently, overlapping signaling of P2ry12 and MHC class II was also detected in the microglia of EAU (Fig. 6C). These results suggest that minocycline treatment can reduce the MHC class II expression by the resident and infiltrating cells in the retina.

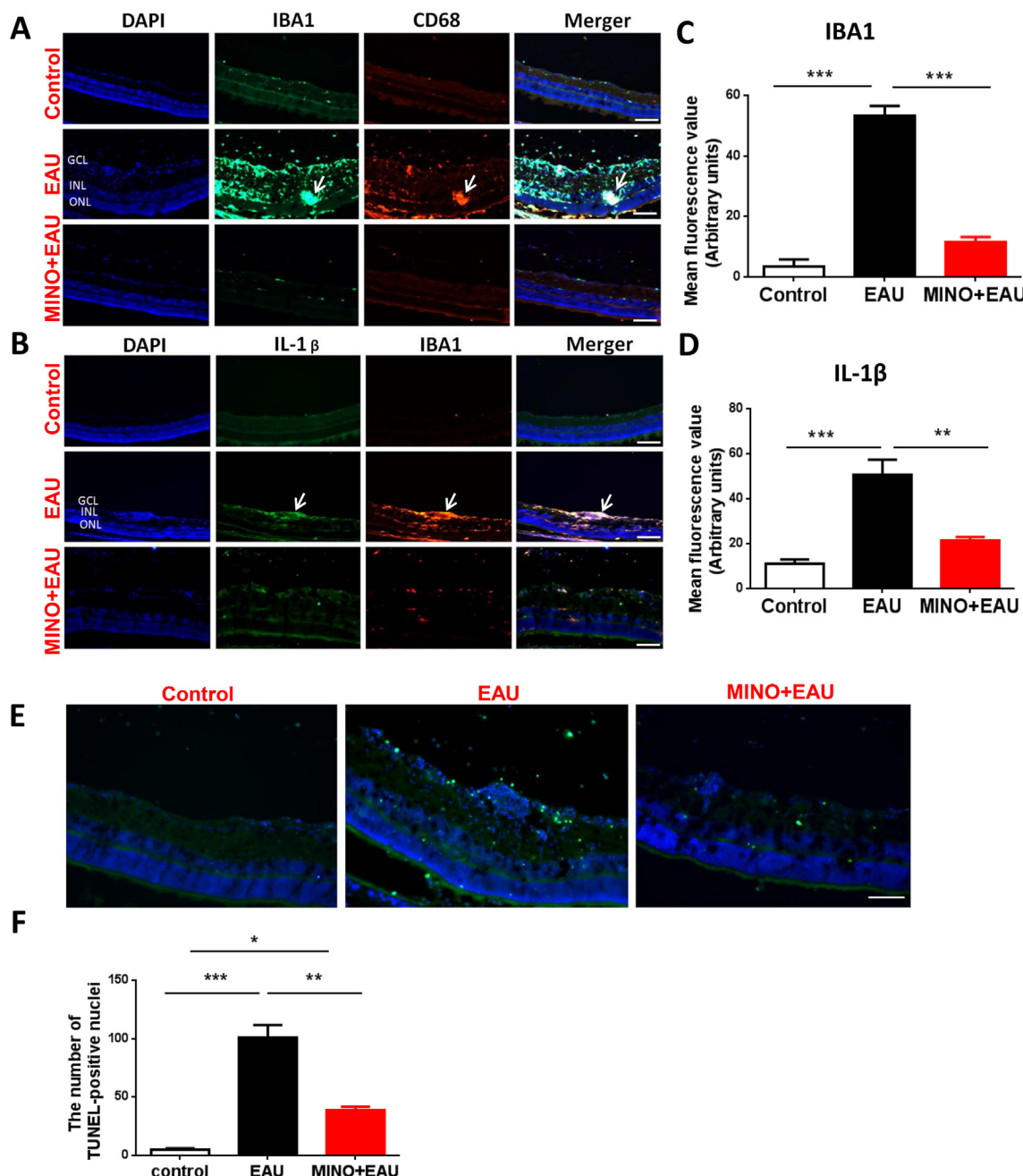


**Fig. 3.** Minocycline treatment suppressed the microglial activity and downregulated retinal IL-1 $\beta$  level. On D14 after immunization, cryosections from three groups were prepared and stained with various primary antibodies. The representative images of each group were chosen from three or more rats (top panel – control; middle panel – EAU; bottom panel – MINO + EAU). (A) Co-labeled cryosections showing IBA1 (green – a marker for microglia and macrophages) and CD68 (red – a commonly used marker of activated microglia and macrophages). Cell nuclei were stained with DAPI (blue). (B) Co-labeled cross-sections showing IBA1 (red) and IL-1 $\beta$  (green). Cell nuclei were stained with DAPI (blue). (C) The mean fluorescence value of IBA1 among the three groups. (D) The mean fluorescence value of IL-1 $\beta$  among the three groups. (E) The rat retinal cell apoptosis at D14 was evaluated by TUNEL staining. (F) The mean number of TUNEL-positive nuclei among the three groups. Values expressed as mean  $\pm$  SEM and analyzed by one-way ANOVA, followed by Tukey's multiple comparison test ( $n \geq 3$ ; \* –  $p < 0.05$ ; \*\* –  $p < 0.01$ ; \*\*\* –  $p < 0.001$ ; OPL – outer plexiform layer; IPL – inner plexiform layer; INL – inner nuclear layer; ONL – outer nuclear layer; GCL – ganglion cell layer). Scale bars: 50  $\mu$ m. (For interpretation of the references to color in this figure legend, the reader is referred to the web version of this article.)

### 3.7. Minocycline remodeled the intestinal microbial and metabolic composition

Minocycline is a second-generation semisynthetic tetracycline, and gut microbiota has been proven to play a critical role in modulating autoimmune diseases, including EAU. Thus, the collected rat feces were subjected to 16S ribosomal RNA sequencing analysis. The Venn diagram showed that EAU had 82 unique and 870 overlapping OUTS

(operational taxonomic units) with the control. After minocycline treatment, the number of OUTS shared with the PBS-treated EAU group was 845, while the number of exclusive OUTS was 29 (Fig. 7A). A similar analysis by PGMA (weighted pair-group method with arithmetic mean) demonstrated that the three groups had a distinct similarity in the relative abundance in the phylum level (Fig. 7B). Linear discriminant effect size (LEfSe) analysis indicated that the immunization increased the abundance of *Spirochaetes*, *Spirochaetales*, and

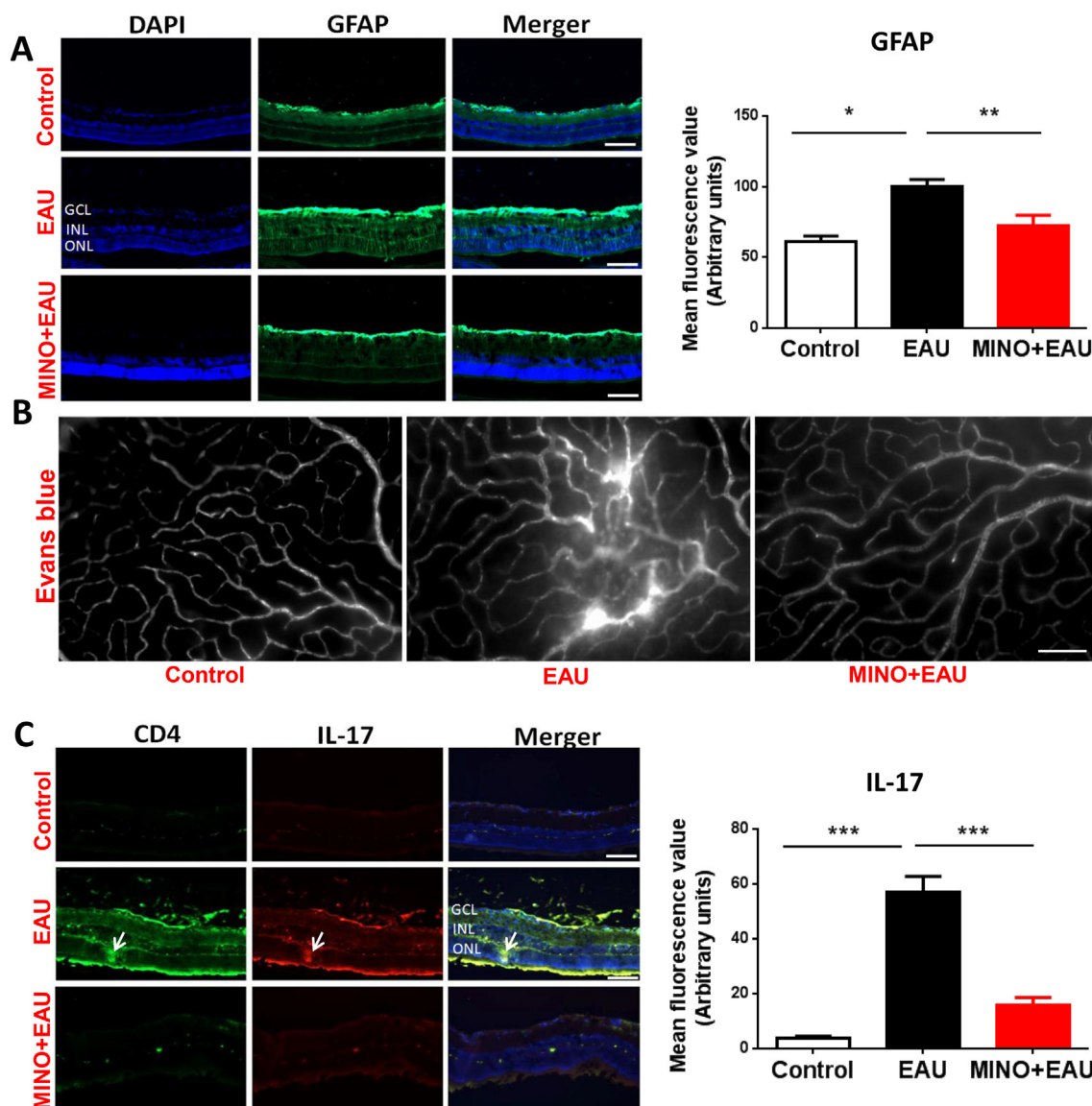


**Fig. 4.** Minocycline preserved the integrity of the blood-retina barrier and inhibited Th17-cell infiltration of the retina. (A and C) On D14 after immunization, cryosections from three groups were prepared and stained with various primary antibodies. The representative images of each group were chosen from three or more rats (top panel – control; middle panel – EAU; bottom panel – MINO + EAU). (A) Immunostaining of cross-sections showing GFAP immunoreactivity among the three groups (left panels; GFAP: a marker for astrocytes and activated Müller cells). The mean fluorescence value of GFAP among the three groups (right panels); (B) Representative images of flat-mounted retinas from each group after perfusion with Evans blue dye to examine the integrity and permeability of blood–retina barrier (BRB) on D14. (C) Co-labeled cryosections showing CD4 (green) and IL-17 (red) immunoreactivities among the three groups (left panels). The mean fluorescence value of IL-17 among the three groups (right panels); Values expressed as mean  $\pm$  SEM and analyzed by one-way ANOVA, followed by Tukey's multiple comparison test ( $n \geq 5$ ; \* –  $p < 0.05$ ; \*\* –  $p < 0.01$ ; \*\*\* –  $p < 0.001$ ; OPL – outer plexiform layer; IPL – inner plexiform layer; INL – inner nuclear layer; ONL – outer nuclear layer; GCL – ganglion cell layer). Scale bars: 50  $\mu$ m. (For interpretation of the references to color in this figure legend, the reader is referred to the web version of this article.)

*Spirochaetia*, but decreased the abundance of *Bacilli*, *Lactobacillales*, and *Firmicutes* (LDA score ( $\log_{10}$ )  $> 4$ ) as compared with the control, while the minocycline treatment enriched the abundance of *Bacteroidetes*, *Muribaculaceae* and *Acidaminococcus* (LDA score ( $\log_{10}$ )  $> 4$ ) in the minocycline-treated EAU groups (Fig. 7C). Consistently, the hierarchical clustering analysis also revealed these three groups had dissimilar relative abundance at the genus level (Fig. 7D). Additionally, Metastats analysis (an improved statistical method for analysis of metagenomic data) indicated that EAU significantly increased the relative abundance of *Delta proteobacteria* and *Spirochaetia* at class level (Fig. 7E and 7F) and the relative abundance of *Ruminococcus bromii*, *Streptococcus hyointestinalis* and *Desulfovibrio* sp. ABHU2SB at the species level (Fig. 7G-I), when compared with control groups (all  $p < 0.05$ ). On the

other hand, minocycline supplementation significantly decreased the relative abundance of these bacterial taxa (Fig. 7G-I, all  $p < 0.05$ ). Meanwhile, minocycline administration was associated with a higher abundance of *Parabacteroides goldsteinii* than PBS-treated EAU (Fig. 7J,  $p < 0.05$ ), but immunization did not significantly alter the abundance of *Parabacteroides goldsteinii* compared to the control (Fig. 7J,  $p > 0.05$ ). Together, this evidence suggests that the immunization alters the composition of gut microbiota when compared to the non-immunized rats, while minocycline remodels the architecture of gut microbiota in EAU rats.

To further understand the importance of gut microenvironment composition, an untargeted fecal metabolism analysis was performed by LC-MS/MS. Similarly, the Venn diagram showed that the EAU vs.

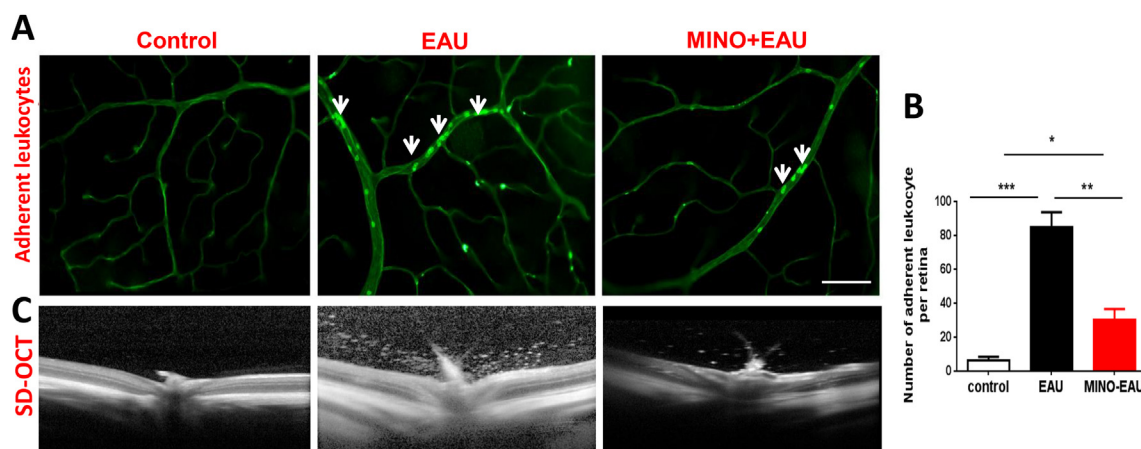


**Fig. 5.** Minocycline reduced retinal leukocyte adhesion and vitreous body infiltrating leukocytes. (A) Representative images of flat-mounted retinas from each group after perfusion with FITC-labeled Con A on D14; the adherent leukocytes indicated by arrows. (B) Mean number of retina-adherent leukocytes in each group ( $n \geq 3$ ). Values expressed as mean  $\pm$  SEM and analyzed by one-way ANOVA, followed by Tukey's multiple comparison test (\* –  $p < 0.05$ ; \*\* –  $p < 0.01$ ; \*\*\* –  $p < 0.001$ ). (C) Representative images of in vivo SD-OCT on D13.

control groups had 157 similar compounds with the MINO + EAU vs. EAU groups, but most metabolites were distinct (Fig. 8A). Volcano plots revealed that the immunization was associated with 472 down-regulated and 265 up-regulated compounds compared to the control (Fig. 8B), while minocycline treatment increased levels of 413 and decreased levels of 186 compounds compared to immunized rats (Fig. 8C). Partial least squares discrimination analysis (PLS-DA) also clearly indicated that the metabolic patterns were largely distinct between EAU vs. control (Fig. 8D, top panel) and MINO + EAU vs. EAU

groups (Fig. 8D, bottom panel). Kyoto encyclopedia of genes and genomes (KEGG) pathway enrichment analysis showed that the immunization significantly affected a variety of biological pathways, primarily linked to carbon metabolism, aminoacyl-tRNA biosynthesis, arginine biosynthesis and alanine, aspartate and glutamate metabolism (Fig. 8E). At the same time, minocycline treatment promoted a functional shift by differentially altering the pathway enrichment compared to the PBS-treated immunized rats, including purine metabolism, inflammatory mediator regulation of TRP channels, and histidine

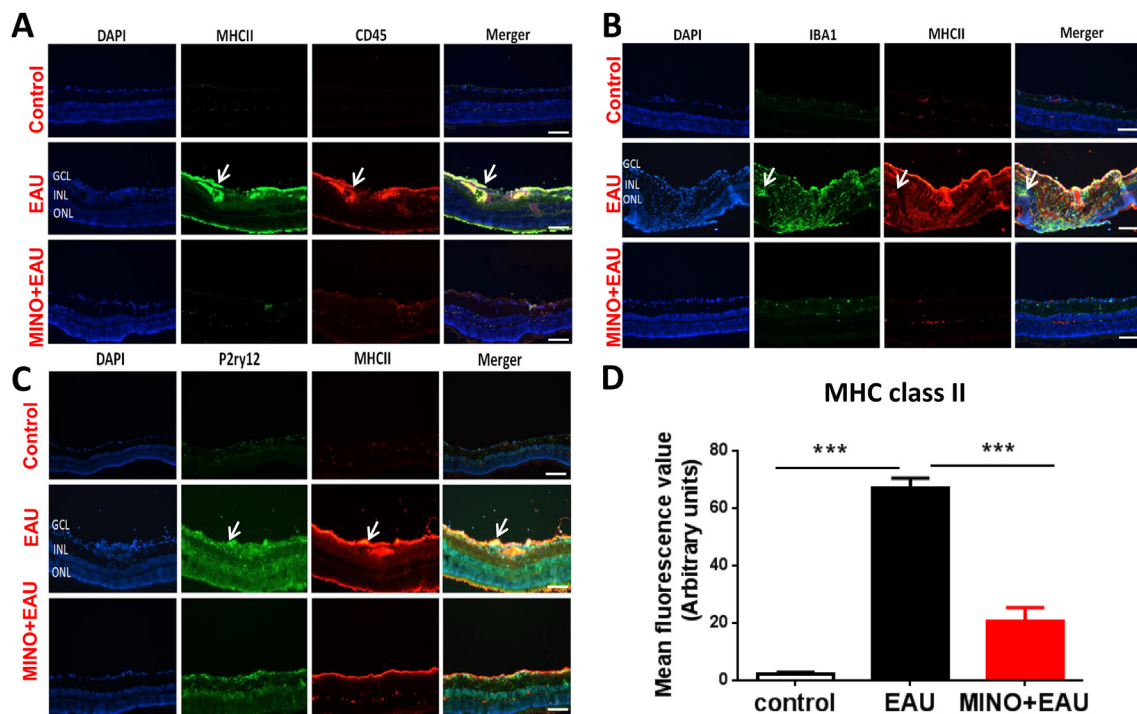


**Fig. 6.** Minocycline decreased MHC class II expression in the retina. On D14 after immunization, cryosections from three groups were prepared and stained with various primary antibodies. The representative images of each group were chosen from three or more rats (top panel – control; middle panel – EAU; bottom panel – MINO + EAU). (A) Immunostaining of cross-sections showing MHC II (green, mostly expressed by antigen-presenting cells) and CD45 (red, a marker for leukocyte). Cell nuclei were stained with DAPI (blue). (B) Immunostaining of cross-sections showing IBA1 (green) and MHC II (red). (C) Immunostaining of cross-sections showing P2ry12 (green, a newly identified selective microglial marker) and MHC II (red). (D) The mean fluorescence value of MHC II among the three groups. Values expressed as mean  $\pm$  SEM and analyzed by one-way ANOVA, followed by Tukey's multiple comparison test ( $n \geq 5$ ; \* –  $p < 0.05$ ; \*\* –  $p < 0.01$ ; \*\*\* –  $p < 0.001$ ; OPL – outer plexiform layer; IPL – inner plexiform layer; INL – inner nuclear layer; ONL – outer nuclear layer; GCL – ganglion cell layer). Scale bars: 50 µm. (For interpretation of the references to color in this figure legend, the reader is referred to the web version of this article.)

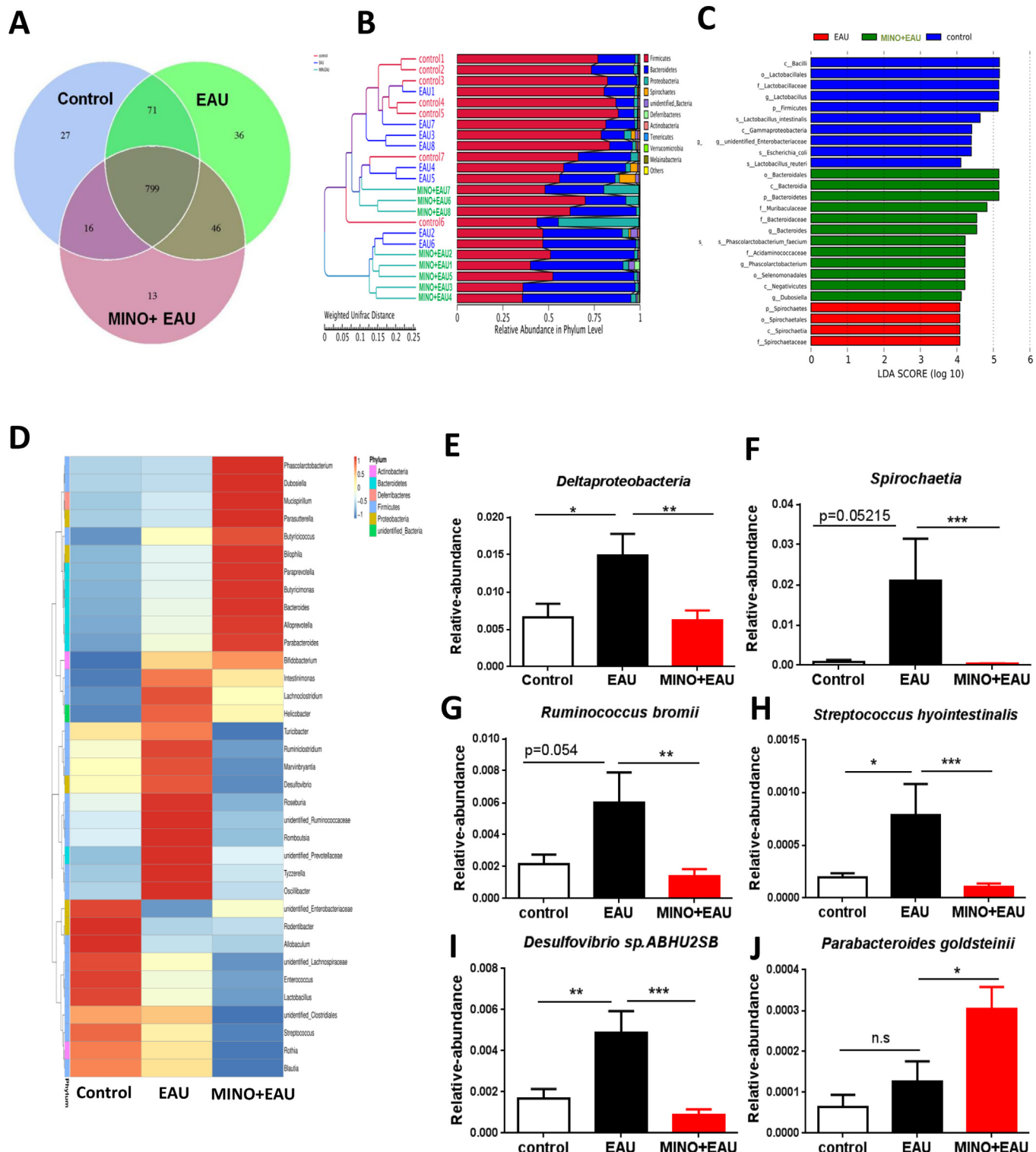


**Fig. 7.** Minocycline remodeled the intestinal microbial composition. (A) The Venn diagram showing the overlapping and unique OTUs (Operational Taxonomic Units) among three groups. (B) A similar analysis of three groups by PGMA (Weighted Pair-group Method with Arithmetic Mean) in the relative abundance at the phylum level. (C) Linear discriminant effect size (LEFSe) analysis for discriminative biomarkers of the gut microbiota among three groups, LDA score ( $\log_{10}$ )  $>$  4. (D) Hierarchical clustering of discriminative relative abundances among three groups at the genus level. Red – relatively high level; blue – relatively low level. (E-J) The relative abundance of control (white), EAU (black), and MINO + EAU (red) at the class and genus levels. (E) *Deltaproteobacteria*; (F) *Spirochaetia*; (G) *Ruminococcus bromii*; (H) *Streptococcus hyointestinalis*; (I) *Desulfovibrio* sp. ABHU2SB; (J) *Parabacteroides goldsteinii*. Values expressed as mean  $\pm$  SEM ( $n = 8$ ) and analyzed by one-way ANOVA, followed by Tukey's multiple comparison test (\* –  $p < 0.05$ ; \*\* –  $p < 0.01$ ; \*\*\* –  $p < 0.001$ ). (For interpretation of the references to color in this figure legend, the reader is referred to the web version of this article.)

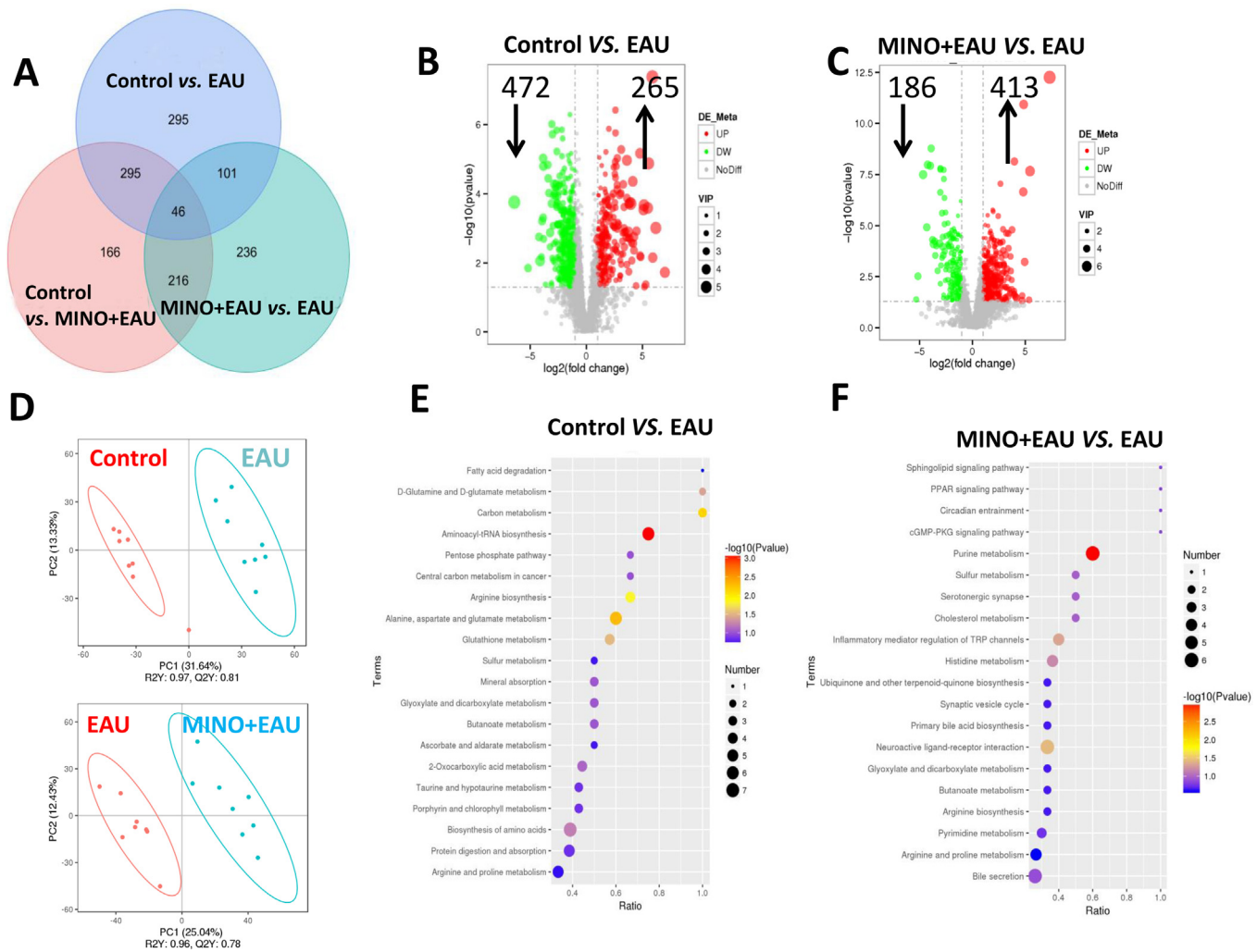


**Fig. 8.** Minocycline treatment changed the level of different intestinal metabolites. (A) Venn diagram showing the overlapping and unique metabolites among the three groups. (B and C) The volcano images of fecal metabolites in control vs. EAU groups (B) and MINO + EAU vs. EAU groups (C). Red plots represent the up-regulated (UP) metabolites, while green plots represent the down-regulated (DW) metabolites. (D) Partial least squares discrimination analysis (PLS-DA) of metabolites in control vs. EAU groups (top panel) and MINO + EAU vs. EAU groups (bottom panel). (E and F) Kyoto encyclopedia of genes and genomes (KEGG) pathway enrichment analysis between control and EAU groups (E) and between MINO + EAU and EAU groups (F). The Y-axis represents the pathway category, and the X-axis represents the degree of pathway enrichment (Rich factor – the number of differently modulated metabolites in each pathway divided by the total number of metabolites involved in that pathway). The color of the circle indicates the p-value and the size of the circle indicates the number of involved metabolites. (G) Hierarchical clustering of metabolites with different levels among three groups. Red – relatively high level; blue – relatively low level. (H-P) Names of metabolites with different levels among control (white), EAU (black), and MINO + EAU (red) groups. (H) L-proline; (I) Allicin; (J) Aceturic acid; (K) Xanthine; (L) Tryptophan; (M) Leukotriene B4; (N) Propionic acid; (O) Histamine; (P) Pantothenic acid. Values expressed as mean  $\pm$  SEM ( $n = 8$ ) and analyzed by one-way ANOVA, followed by Tukey's multiple comparison test (\* –  $p < 0.05$ ; \*\* –  $p < 0.01$ ; \*\*\* –  $p < 0.001$ ). (For interpretation of the references to color in this figure legend, the reader is referred to the web version of this article.)

metabolism (Fig. 8F). The hierarchical clustering analysis of different metabolites identically demonstrated dissimilar patterns of metabolites among these three groups (Fig. 8G). In particular, immunization was associated with decreased relative concentrations of L-proline, allicin, aceturic acid, xanthine, and tryptophan and increased leukotriene B4. However, these changes were reversed by minocycline treatment (Fig. 8H-M,  $p < 0.05$ , one-way ANOVA), except tryptophan (Fig. 8L). Intriguingly, propionic acid, histamine, and pantothenic acid were apparently elevated in the minocycline-treated EAU groups compared to the PBS-treated EAU groups, but PBS-treated EAU groups had levels of those metabolites similar to the control (Fig. 8N-P). All the evidence suggests that the immunization significantly alters the gut metabolic profile, and minocycline treatment promotes a functional shift in gut microenvironment.

### 3.8. Minocycline suppressed the pathological progression of EAU

At last, to determine whether minocycline can suppress the pathological progression of EAU after the onset of the disease, which may provide more meaningful data for clinical treatment, the period of minocycline treatment was changed to D8-D20 (Fig. 9A), since the inflammation has occurred on D8 in this animal model. The clinical assessment indicated that severity of EAU was also markedly attenuated upon minocycline administration in comparison to the PBS-treated EAU (Fig. 9B, the group effect,  $F(1, 55) = 86.54$ ,  $p < 0.001$ ; the significance of the differences on D12, D14, D16 and D18, \*\* $p < 0.01$  and \*\*\* $p < 0.001$ ) and the significantly decreased ocular surface inflammation can be found through slit-lamp observation (Fig. 9C).

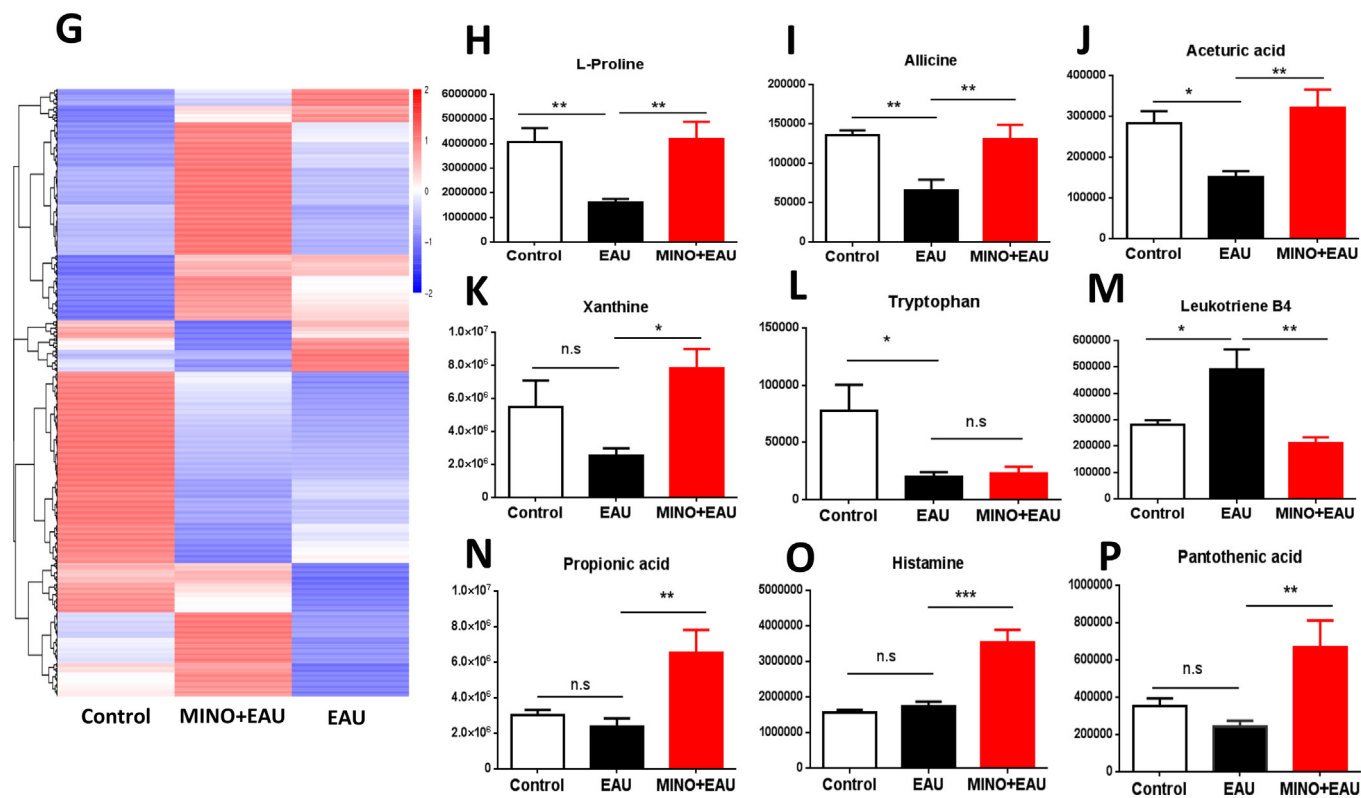


Fig. 8. (continued)

#### 4. Discussion

To the best of our knowledge, this study demonstrates for the first time that minocycline treatment significantly suppresses the initiation and progression of non-infectious uveitis. The protection by minocycline is highly concordant with previous reports indicating that minocycline has protective effects against a variety of retinal diseases, including diabetic retinopathy [24], retinal degeneration [7,25], retinal ischemia [27], branch retinal vein occlusion [29], glaucoma [30], and LPS-induced retinal inflammation [46]. In this study, through clinical and histopathological assessment, minocycline was shown to remarkably reduce the retina inflammation and maintain the normal retinal structure. More importantly, minocycline also can significantly improve the retinal function by preserving normal dark and light-adapted retinal responses which were seriously impaired in the immunized rats. Consistently, minocycline has been shown to improve the

impaired retinal function in animal models of human retinitis pigmentosa, light-induced retinal degeneration, and diabetic retinopathy [7,47,48]. All the evidence suggests that the minocycline treatment histologically and functionally ameliorates the non-infectious uveitis.

Subsequently, we found that the IBA1-labeled microglia/macrophages were highly activated, with larger cell bodies and amoeboid shape (even extended into the outer nuclear layer) on the D14 after immunization. These pathological changes are in line with previous works showing that the IBA1-labeled microglia/macrophages migrated to the outer retina of EAU animals [9,49,50]. The activated state of microglia was verified by co-labeling with CD68 (a microglia activated marker), and the highly overlapping signaling strongly indicated that the microglia in the non-infection uveitis were overactive. The activated microglia capable of releasing pro-inflammatory cytokines were considered as the main pathological factors of various retinal diseases. In our study, the activated microglia were significantly silenced, and IL-

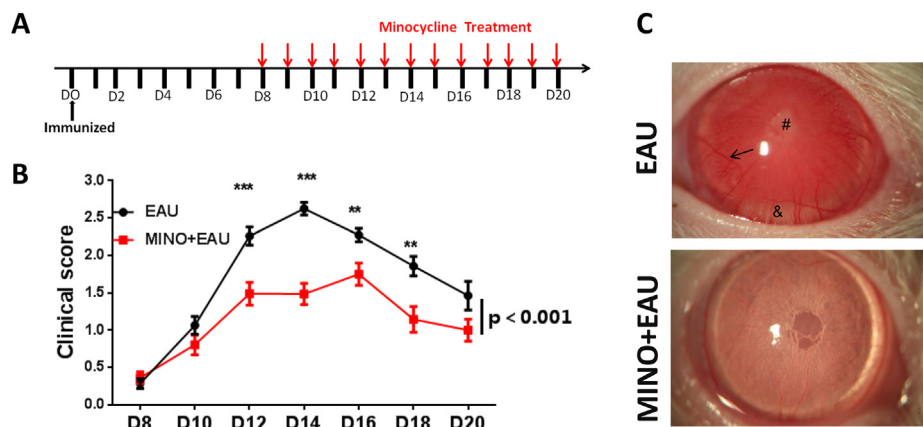


**Fig. 9.** Minocycline suppressed the progression of experimental autoimmune uveitis after the inflammation onset. (A) The schematic time course of minocycline treatment from D8 to D20. (B) Time course of EAU clinical scores ( $n \geq 12$  rats per group) as determined by slit-lamp observation. EAU group (black) treated with the same volume of PBS as minocycline treatment; MINO + EAU (red) group was injected with 50 mg/kg minocycline per day. Two-way ANOVA for repeated measures with post hoc Bonferroni's test was used for the comparison of clinical score data. (C) Representative ocular images by slit-lamp observation on D16. Dilated vessels ( $\rightarrow$ ), severe hypopyon (&), and massive leakage of inflammatory cells (#) were observed in EAU. All the data expressed as mean  $\pm$  SEM ( $n \geq 12$ ; \* –  $p < 0.05$ ; \*\* –  $p < 0.01$ ; \*\*\* –  $p < 0.001$ ). (For interpretation of the references to color in this figure legend, the reader is referred to the web version of this article.)

$1\beta$  released by microglia/macrophages was also evidently decreased following minocycline administration. IL-1 $\beta$  is a pro-inflammatory cytokine implicated in many retinal pathologies as well as autoimmune diseases by causing neuroinflammation, cytotoxicity, pyroptosis, and mitochondrial dysfunction [51]. Moreover, upregulated IL-1 $\beta$  can enhance the leukocyte infiltration by increasing the expression of adhesion molecules and damaging the blood-retinal barrier (BRB) [52], which is in line with our results shown in Fig. 4B and Fig. 5. The GFAP-immunoreactivity was markedly increased and expanded over the whole retina, and, given that GFAP protein is a marker of astrocytes and activated Müller cells, its over-activation indicated the disruption of the BRB [45]. Indeed, our Evans blue test showed that the immunized retinas were filled with Evans blue dye, but minocycline preserved the integrity and inhibited the permeability of the BRB, which is indicated by less Evans blue leakage and less infiltrating macrophages and T-cells observed in our study (Fig. 4 and Fig. 5). Concordant results were found in retinal ischemia-reperfusion injury and intracerebral hemorrhage following minocycline treatment [53,54]. Along with the increased level of invading T-cells, the number of Th17 cells co-labeled with IL-17 and CD4 was concurrently growing, Th17 cells were considered as the main contributor to the autoimmune uveitis, and minocycline significantly reduced the Th17 influx (Fig. 4C). Meanwhile, the activated microglia were reported to trigger leukocytes adhesion to retinal vessels and recruit inflammatory cells into the retina [11]. Indeed, using perfusion with FITC-Con A lectin, a large number of adherent leukocytes were observed in the immunized retinal vessels. Moreover, *in vivo* images by SD-OCT similarly revealed a large number of intravitreal leukocytes (Fig. 5). As expected, minocycline effectively reduced the number of inherent leukocytes and suppressed the recruitment of inflammatory cells into the retina. Additionally, retinal antigen-presenting cells (indicated by MHC II expression) can drive the development and progression of EAU disease [9]. In this work, we demonstrated an intensive upregulation of MHC class II expression across the whole immunized retina, and an apparent decrease of the MHC II expression after minocycline administration. Interestingly, we found that MHC II was strongly expressed by CD45-positive cells and partially colocalized with IBA1-expressing microglia/macrophages and P2ry12-selectively expressing microglia in the EAU retinas. These findings are in line with previous evidence showing that MHC class II was mostly expressed by infiltrating antigen-presenting cells (APCs) such as monocytes, macrophages, and dendritic cells [9,55], and also consistent with the evidence demonstrating that the retina-resident activated microglia can express the MHC II as local APCs driving the development of intraocular inflammation [56]. However, our results contradict the findings of Connor's group, who recently showed that the resident activated microglia were MHC II-negative in mice EAU model, and microglia-mediated infiltration of inflammatory cells was antigen-nonspecific [11]. In all, our evidence demonstrates that minocycline can attenuate EAU development by suppressing the microglial activation. Herein, we have to mention that although reactive microglia have been identified in most of the retinal pathologies, microglia seem to have a double-edged role with its both proinflammatory and anti-inflammatory functions [57]. For example, removal of microglia seriously aggravated retinal degeneration in ocular hypertension, corneal penetration and chemical injury by significant upregulation of major inflammatory factors [58]. So, there were no consensus effects of microglia in ocular diseases, and they seem to be condition-dependent. Therefore, more systemic and careful research is still needed to delineate the role of microglia in all kinds of retinal diseases.

Since minocycline is a broad-spectrum antibiotic, and dysfunction of gut homeostasis has been implicated in many central nervous system diseases and retinal diseases, including Parkinson's disease (PD), Alzheimer's disease (AD), amyotrophic lateral sclerosis (ALS), diabetic retinopathy (DR), glaucoma and EAU [18–20,22,59–62]. The role of gut microbiota in the EAU also has been deeply explored in the last decades. Consistent with previous evidence, we found that the gut

microbial composition in immunized rats was also tremendously altered compared to the control rats, and similar alteration can be found in the EAU mice model, clinical Behcet's disease and Vogt-Koyanagi-Harada disease [18–20,60]. Disappointedly, we failed to identify the same pathogenic bacteria as the clinical Behcet's disease and Vogt-Koyanagi-Harada disease. Nevertheless, in our study, the abundances of *Desulfovibrio*, *Ruminococcus bromii*, *Streptococcus hyointestinalis* and pathogenic *Spirochaeta* in guts of the immunized rats were much higher than in the control group; the increased *Desulfovibrio*, a sulfate-reducing bacteria (SRB), was implicated in the development of inflammation in colitis by triggering Th17 cell activation [63]. *Ruminococcus bromii* was negatively correlated with fecal levels of the main short-chain fatty acids (SCFAs) in the human gut (i.e., acetate, butyrate, and propionate) [64]. By contrast, *Streptococcus hyointestinalis* was positively correlated with neuroinflammation [65]. Following minocycline treatment, the relative abundances of these bacteria were evidently decreased. Additionally, minocycline supplementation can enhance the enrichment of *Parabacteroides goldsteinii*, which has been proven to reduce the levels of IL-1 $\beta$  and TNF- $\alpha$  and maintain intestinal permeability [66,67], although the immunized rats had an abundance of *Parabacteroides goldsteinii* similar to the control. This evidence suggests that the gut microbiota was altered by the EAU, but minocycline treatment remodeled the gut microbial composition. Resembling results were also obtained by fecal metabolomic analysis. The gut metabolic profile was significantly altered after disease, including the gut microbiota-derived SCFAs and tryptophan metabolites. Among these changes, the EAU tremendously decreased the levels of L-proline, allixin, aceturic acid, and tryptophan and increased the level of leukotriene B4 compared to the control. Conversely, minocycline elevated the concentrations of L-proline, allixin, aceturic acid, and xanthine, which, as immunomodulators, play an important role in keeping intestinal permeability and reducing the pro-inflammatory cytokines (such as IL-1 $\beta$  and IL-17) [68–71]. Meanwhile, minocycline reduced EAU-increased leukotriene B4 level, which was positively correlated with the recruitment and activation of neutrophils, production of proinflammatory cytokines, and migration of Th17 cells [72]. More importantly, blocking the interaction of leukotriene B4 with its receptor has been shown to markedly suppress the development and progression of EAU in the mouse model [73]. Additionally, the minocycline-upregulated propionic acid, histamine, and pantothenic acid have various immunomodulatory effects such as diminishing TNF- $\alpha$  and IL-1 $\beta$  [74–76]. This evidence demonstrates that the minocycline can modulate the function of the intestinal microenvironment.

Based on current evidence that depletion of commensal microbiota by antibiotics or rearing under the germ-free conditions can markedly decrease the severity of autoimmune inflammation in antigen-immunized EAU or spontaneous uveitis model in R161H mice [20,21,77], and that minocycline was shown to be able to modulate depressive disorder by changing the microbial composition [31,32], we speculate that functional shift in gut homeostasis induced by minocycline is also, at least partially, responsible for the minocycline-induced protection against EAU disease, but we have to admit that more data is still required to confirm it. Moreover, after the inflammation onset of EAU, the minocycline treatment can also significantly attenuate the disease progression (Fig. 9). These results are in line with the effects of minocycline in the experimental autoimmune encephalomyelitis (EAE) [78,79] but contradict the effects of retinal microglia removal in EAU [11]. The former evidence shows that minocycline treatment can delay and suppress the EAE onset and progression when minocycline is administered at different periods. The latter evidence indicates that suppression of EAU via elimination of retinal microglia is time-dependent: removal of microglia at the early stages of EAU prevents uveitis from initiation but has little effect upon removal of microglia at the later stages. This divergence, in our opinion, may be attributed to the minocycline-induced functional shift in the gut microenvironment.

Although we suggested that minocycline suppressed the EAU by a

combination of inhibiting local microglial activation and shifting intestinal function, we admitted that only by measuring the concentration of minocycline in the eye and intestine would allow us to explicitly interpret whether the observed effects induced by systemic minocycline treatment were attributed to directly inhibit the retinal microglial activation or remodel the gut microenvironment, or a combination of both, and by comparing the tissue concentration after the two different doses treatment, we also could further examine whether the observed dose-dependent efficacy was dose-exposure-dependent or not. Only this specific research can provide a better understanding of the mechanism underlying the initiation and progression of EAU, although some studies had already been done to verify these notions. For example, oral administration of gut microbiota-derived SCFAs, including propionate and butyrate, significantly attenuated the uveitis severity [80] and genetic deletion of the local microglia inhibited the initiation of EAU. However, in this work, the challenge we faced in local pharmacological inhibition of microglial activation seems to be hard to overcome since multiple intravitreal injections are not allowed because of severe side effects, but our and other recent works using nano-biomaterials provided a promising solution. For example, we found that a single intravitreal injection of dexamethasone supramolecular hydrogel significantly attenuated the inflammatory response in rat non-infectious uveitis without any undesirable side effects [81]. Luo et al. observed that the controlled release of biodegradable nanoparticles wrapping -corticosteroid via one subconjunctival injection evidently reduced the clinical score of rat EAU. These research shed some light on how to achieve regional pharmacological inhibition of microglia [82].

In summary, our results suggest that minocycline treatment can mitigate the development and progression of experimental autoimmune uveitis via inhibiting the retinal microglial activation and remodeling the function of the intestinal microenvironment. Combined with the well-known safety of minocycline in various clinical experiments [33,34], we assert that minocycline may serve as a safe, inexpensive, and efficient therapy for clinical uveitis.

#### CRediT authorship contribution statement

**Jianhong Zhou:** Conceptualization, Investigation, Data curation, Writing - review & editing. **Jingjing Yang:** Investigation. **Mali Dai:** Investigation, Funding acquisition. **Dan Lin:** Investigation. **Renshu Zhang:** Visualization, Investigation, Validation. **Hui Liu:** Validation. **Ailing Yu:** Investigation. **Serhii Vakal:** Conceptualization, Writing - original draft, Writing - review & editing. **Yuqin Wang:** Project administration, Funding acquisition, Writing - review & editing, Supervision, Funding acquisition. **Xingyi Li:** Conceptualization, Writing - original draft, Writing - review & editing, Funding acquisition, Supervision.

#### Declaration of Competing Interest

The authors declare that they have no known competing financial interests or personal relationships that could have appeared to influence the work reported in this paper.

#### Acknowledgements

This work was supported by the National Natural Science Foundation of China (81971732 and 31671022); the Zhejiang Provincial Natural Science Foundation of China (LQ20H180006 and LR18H30002); the Innovation Research Program of the Eye Hospital (YNCX201608); Wenzhou Science and Technology Foundation (No. Y20190625).

#### References

- [1] S. Bansal, V.A. Barathi, D. Iwata, R. Agrawal, Experimental autoimmune uveitis and other animal models of uveitis: An update, *Indian J. Ophthalmol.* 63 (3) (2015) 211–218.
- [2] D.C. Gritz, I.G. Wong, Incidence and prevalence of uveitis in Northern California; the Northern California Epidemiology of Uveitis Study, *Ophthalmology* 111 (3) (2004).
- [3] H. Goto, M. Mochizuki, K. Yamaki, S. Kotake, M. Usui, S. Ohno, Epidemiological survey of intraocular inflammation in Japan, *Jpn. J. Ophthalmol.* 51 (1) (2007) 41–44.
- [4] O.M. Durrani, N.N. Tehrani, J.E. Marr, P. Moradi, P. Stavrou, P.I. Murray, Degree, duration, and causes of visual loss in uveitis, *British J. Ophthalmol.* 88 (9) (2004) 1159–1162.
- [5] C. Balser, A. Wolf, M. Herb, T. Langmann, Co-inhibition of PGF and VEGF blocks their expression in mononuclear phagocytes and limits neovascularization and leakage in the murine retina, *J. Neuroinflam.* 16 (1) (2019) 26.
- [6] Y. Okunuki, R. Mukai, E.A. Pearsall, G. Klokman, D. Husain, D.H. Park, E. Korobkina, H.L. Weiner, O. Butovsky, B.R. Ksander, J.W. Miller, K.M. Connor, Microglia inhibit photoreceptor cell death and regulate immune cell infiltration in response to retinal detachment, *PNAS* 115 (27) (2018) E6264–E6273.
- [7] B. Peng, J. Xiao, K. Wang, K.F. So, G.L. Tipoe, B. Lin, Suppression of microglial activation is neuroprotective in a mouse model of human retinitis pigmentosa, *The Journal of Neuroscience : the official journal of the Society for Neuroscience* 34(24) (2014) 8139–50.
- [8] C. Altmann, M.H.H. Schmidt, The Role of Microglia in Diabetic Retinopathy: Inflammation, Microvasculature Defects and Neurodegeneration, *Int. J. Mol. Sci.* 19 (1) (2018).
- [9] D.A. Lipski, R. Dewispelaere, V. Foucart, L.E. Caspers, M. Defrance, C. Bruyns, F. Willermain, MHC class II expression and potential antigen-presenting cells in the retina during experimental autoimmune uveitis, *J. Neuroinflam.* 14 (1) (2017) 136.
- [10] Y. Huang, J. He, H. Liang, K. Hu, S. Jiang, L. Yang, S. Mei, X. Zhu, J. Yu, A. Kijlstra, P. Yang, S. Hou, Aryl Hydrocarbon Receptor Regulates Apoptosis and Inflammation in a Murine Model of Experimental Autoimmune Uveitis, *Front. Immunol.* 9 (2018) 1713.
- [11] Y. Okunuki, R. Mukai, T. Nakao, S.J. Tabor, O. Butovsky, R. Dana, B.R. Ksander, K.M. Connor, Retinal microglia initiate neuroinflammation in ocular autoimmunity, *PNAS* 116 (20) (2019) 9989–9998.
- [12] J.G. Lee, D.S. Han, S.V. Jo, A.R. Lee, C.H. Park, C.S. Eun, Y. Lee, Characteristics and pathogenic role of adherent-invasive Escherichia coli in inflammatory bowel disease: Potential impact on clinical outcomes, *PLoS ONE* 14 (4) (2019) e0216165.
- [13] C. Palmela, C. Chevarin, Z. Xu, J. Torres, G. Sevrin, R. Hirten, N. Barnich, S.C. Ng, J.F. Colombel, Adherent-invasive Escherichia coli in inflammatory bowel disease, *Gut* 67 (3) (2018) 574–587.
- [14] X.M. Luo, M.R. Edwards, Q. Mu, Y. Yu, M.D. Vieson, C.M. Reilly, S.A. Ahmed, A.A. Bankole, Gut Microbiota in Human Systemic Lupus Erythematosus and a Mouse Model of Lupus, *Appl. Environ. Microbiol.* 84 (4) (2018).
- [15] X. Zhang, D. Zhang, H. Jia, Q. Feng, D. Wang, D. Liang, X. Wu, J. Li, L. Tang, Y. Li, Z. Lan, B. Chen, Y. Li, H. Zhong, H. Xie, Z. Jie, W. Chen, S. Tang, X. Xu, X. Wang, X. Cai, S. Liu, Y. Xia, J. Li, X. Qiao, J.Y. Al-Aama, H. Chen, L. Wang, Q.J. Wu, F. Zhang, W. Zheng, Y. Li, M. Zhang, G. Luo, W. Xue, L. Xiao, J. Li, W. Chen, X. Xu, Y. Yin, H. Yang, J. Wang, K. Kristiansen, L. Liu, T. Li, Q. Huang, Y. Li, J. Wang, The oral and gut microbiomes are perturbed in rheumatoid arthritis and partly normalized after treatment, *Nat. Med.* 21 (8) (2015) 895–905.
- [16] F. Chu, M. Shi, Y. Lang, D. Shen, T. Jin, J. Zhu, L. Cui, Gut Microbiota in Multiple Sclerosis and Experimental Autoimmune Encephalomyelitis: Current Applications and Future Perspectives, *Mediators Inflamm.* 2018 (2018) 8168717.
- [17] S. Jangi, R. Gandhi, L.M. Cox, N. Li, F. von Glehn, R. Yan, B. Patel, M.A. Mazzola, S. Liu, B.L. Glanz, S. Cook, S. Tankou, F. Stuart, K. Melo, P. Nejad, K. Smith, B.D. Topcuolu, J. Holden, P. Kivisakk, T. Chitnis, P.L. De Jager, F.J. Quintana, G.K. Gerber, L. Bry, H.L. Weiner, Alterations of the human gut microbiome in multiple sclerosis, *Nat. Commun.* 7 (2016) 12015.
- [18] Z. Ye, N. Zhang, C. Wu, X. Zhang, Q. Wang, X. Huang, L. Du, Q. Cao, J. Tang, C. Zhou, S. Hou, Y. He, Q. Xu, X. Xiong, A. Kijlstra, N. Qin, P. Yang, A metagenomic study of the gut microbiome in Behcet's disease, *Microbiome* 6 (1) (2018).
- [19] Z. Ye, C. Wu, N. Zhang, L. Du, Q. Cao, X. Huang, J. Tang, Q. Wang, F. Li, C. Zhou, Q. Xu, X. Xiong, A. Kijlstra, N. Qin, P. Yang, Altered gut microbiome composition in patients with Vogt-Koyanagi-Harada disease, *Gut Microbes* (2020) 1–17.
- [20] Y.K. Nakamura, C. Metea, L. Karstens, M. Asquith, H. Gruner, C. Moscibroicki, I. Lee, C.J. Brislawn, J.K. Jansson, J.T. Rosenbaum, P. Lin, Gut Microbial Alterations Associated With Protection From Autoimmune Uveitis, *Invest. Ophthalmol. Vis. Sci.* 57 (8) (2016) 3747–3758.
- [21] J. Heissigerova, P. Seidler Stangova, A. Klimova, P. Svozilkova, T. Hrnccir, R. Stepankova, M. Kverka, H. Tlaskalova-Hogenova, J.V. Forrester, The Microbiota Determines Susceptibility to Experimental Autoimmune Uveoretinitis, *Journal of immunology research* 2016 (2016) 5065703.
- [22] C.R. Zarate-Blades, R. Horai, M.J. Mattapallil, N.J. Ajami, M. Wong, J.F. Petrosino, K. Itoh, C.C. Chan, R.R. Caspi, Gut microbiota as a source of a surrogate antigen that triggers autoimmunity in an immune privileged site, *Gut Microbes* 8 (1) (2017) 59–66.
- [23] K. Maier, D. Merkler, J. Gerber, N. Taheri, A.V. Kuhnert, S.K. Williams, C. Neusch, M. Bahr, R. Diem, Multiple neuroprotective mechanisms of minocycline in autoimmune CNS inflammation, *Neurobiol. Dis.* 25 (3) (2007) 514–525.
- [24] W. Wang, S. Sidoli, W. Zhang, Q. Wang, L. Wang, O.N. Jensen, L. Guo, X. Zhao, L. Zheng, Abnormal levels of histone methylation in the retinas of diabetic rats are

- reversed by minocycline treatment, *Sci. Rep.* 7 (2017) 45103.
- [25] R. Scholz, M. Sobotka, A. Caramoy, T. Stempf, C. Moehle, T. Langmann, Minocycline counter-regulates pro-inflammatory microglia responses in the retina and protects from degeneration, *J. Neuroinflamm.* 12 (2015) 209.
- [26] J. Di Pierdomenico, R. Scholz, F.J. Valiente-Soriano, M.C. Sanchez-Migallon, M. Vidal-Sanz, T. Langmann, M. Agudo-Barriuso, D. Garcia-Ayuso, M.P. Villegas-Perez, Neuroprotective Effects of FGF2 and Minocycline in Two Animal Models of Inherited Retinal Degeneration, *Invest. Ophthalmol. Vis. Sci.* 59 (11) (2018) 4392–4403.
- [27] A. Ahmed, L.L. Wang, S. Abdelmaksoud, A. Aboelgheit, S. Saeed, C.L. Zhang, Minocycline modulates microglia polarization in ischemia-reperfusion model of retinal degeneration and induces neuroprotection, *Sci. Rep.* 7 (1) (2017) 14065.
- [28] R. Huang, S. Liang, L. Fang, M. Wu, H. Cheng, X. Mi, Y. Ding, Low-dose minocycline mediated neuroprotection on retinal ischemia-reperfusion injury of mice, *Mol. Vision* 24 (2018) 367–378.
- [29] C. Sun, X.X. Li, X.J. He, Q. Zhang, Y. Tao, Neuroprotective effect of minocycline in a rat model of branch retinal vein occlusion, *Exp. Eye Res.* 113 (2013) 105–116.
- [30] H. Levkovich-Verbin, Y. Waserzoog, S. Vander, D. Makarovsky, I. Piven, Minocycline upregulates pro-survival genes and downregulates pro-apoptotic genes in experimental glaucoma, Graefes archive for clinical and experimental ophthalmology = Albrecht von Graefes Archiv fur klinische und experimentelle, *Ophthalmologie* 252 (5) (2014) 761–772.
- [31] M.L. Wong, A. Inserra, M.D. Lewis, C.A. Mastronardi, L. Leong, J. Choo, S. Kentish, P. Xie, M. Morrison, S.L. Wesselingh, G.B. Rogers, J. Licinio, Inflammasome signaling affects anxiety- and depressive-like behavior and gut microbiome composition, *Mol. Psych.* 21 (6) (2016) 797–805.
- [32] A.K. Schmidtn, D.A. Slattery, J. Glasner, A. Hiergeist, K. Gryksa, V.A. Malik, J. Hellmann-Regen, I. Heuser, T.C. Baghai, A. Gessner, R. Rupprecht, B. Di Benedetto, I.D. Neumann, Minocycline alters behavior, microglia and the gut microbiome in a trait-anxiety-dependent manner, *Transl. Psych.* 9 (1) (2019) 223.
- [33] J.D. Rosenblat, R.S. McIntyre, Efficacy and tolerability of minocycline for depression: A systematic review and meta-analysis of clinical trials, *J. Affect. Disord.* 227 (2018) 219–225.
- [34] L. Zhang, H. Zheng, R. Wu, T.R. Kosten, X.Y. Zhang, J. Zhao, The effect of minocycline on amelioration of cognitive deficits and pro-inflammatory cytokines levels in patients with schizophrenia, *Schizophr. Res.* 212 (2019) 92–98.
- [35] W. Wu, Z. He, Z. Zhang, X. Yu, Z. Song, X. Li, Intravitreal injection of rapamycin-loaded polymeric micelles for inhibition of ocular inflammation in rat model, *Int. J. Pharm.* 513 (1–2) (2016) 238–246.
- [36] I. Van Hoeve, E. Lefevere, L. De Groef, J. Sergeys, M. Salinas-Navarro, C. Libert, R. Vandebroucke, L. Moons, MMP-3 Deficiency Alleviates Endotoxin-Induced Acute Inflammation in the Posterior Eye Segment, *Int. J. Mol. Sci.* 17 (11) (2016).
- [37] T. Yan, W. Xiong, F. Huang, F. Zheng, H. Ying, J.F. Chen, J. Qu, X. Zhou, Daily Injection But Not Continuous Infusion of Apomorphine Inhibits Form-Depression Myopia in Mice, *Invest. Ophthalmol. Vis. Sci.* 56 (4) (2015) 2475–2485.
- [38] F. Qiu, G. Matlock, Q. Chen, K. Zhou, Y. Du, X. Wang, J.X. Ma, Therapeutic Effects of PPAR $\alpha$  Agonist on Ocular Neovascularization in Models Recapitulating Neovascular Age-Related Macular Degeneration, *Invest. Ophthalmol. Vis. Sci.* 58 (12) (2017) 5065–5075.
- [39] L. Sun, H. Jia, J. Li, M. Yu, Y. Yang, D. Tian, H. Zhang, Z. Zou, Cecal Gut Microbiota and Metabolites Might Contribute to the Severity of Acute Myocardial Ischemia by Impacting the Intestinal Permeability, Oxidative Stress, and Energy Metabolism, *Front. Microbiol.* 10 (2019).
- [40] J. Lu, X. Zhang, Y. Liu, H. Cao, Q. Han, B. Xie, L. Fan, X. Li, J. Hu, G. Yang, X. Shi, Effect of Fermented Corn-Soybean Meal on Serum Immunity, the Expression of Genes Related to Gut Immunity Gut Microbiota, and Bacterial Metabolites in Grower-Finisher Pigs, *Front. Microbiol.* 10 (2019) 2620.
- [41] J.G. Caporaso, J. Kuczynski, J. Stombaugh, K. Bittinger, F.D. Bushman, E.K. Costello, N. Fierer, A.G. Pena, J.K. Goodrich, J.I. Gordon, G.A. Hutte, S.T. Kelley, D. Knights, J.E. Koenig, R.E. Ley, C.A. Lozupone, D. McDonald, B.D. Mueggel, M. Pirrung, J. Reeder, J.R. Sevinsky, P.J. Turnbaugh, W.A. Walters, J. Widmann, T. Yatsunenko, J. Zaneveld, R. Knight, QIIME allows analysis of high-throughput community sequencing data, *Nat. Methods* 7 (5) (2010) 335–336.
- [42] R.C. Edgar, B.J. Haas, J.C. Clemente, C. Quince, R. Knight, UCHIME improves sensitivity and speed of chimera detection, *Bioinformatics* 27 (16) (2011) 2194–2200.
- [43] R.C. Edgar, UPARSE: highly accurate OTU sequences from microbial amplicon reads, *Nat. Methods* 10 (10) (2013) 996–998.
- [44] R.C. Edgar, MUSCLE: multiple sequence alignment with high accuracy and high throughput, *Nucleic Acids Res.* 32 (5) (2004) 1792–1797.
- [45] E. Vecino, F.D. Rodriguez, N. Ruzaña, X. Pereiro, S.C. Sharma, Glia-neuron interactions in the mammalian retina, *Progress in retinal and eye research* 51 (2016) 1–40.
- [46] Z. Yuan, X. Chen, W. Yang, B. Lou, N. Ye, Y. Liu, The anti-inflammatory effect of minocycline on endotoxin-induced uveitis and retinal inflammation in rats, *Mol. Vision* 25 (2019) 359–372.
- [47] Y. Wu, Y. Chen, Q. Wu, L. Jia, X. Du, Minocycline inhibits PARP1 expression and decreases apoptosis in diabetic retinopathy, *Mol. Med. Rep.* 12 (4) (2015) 4887–4894.
- [48] C. Zhang, B. Lei, T.T. Lam, F. Yang, D. Sinha, M.O.M. Tso, Neuroprotection of Photoreceptors by Minocycline in Light-Induced Retinal Degeneration, *Investig. Ophthalmol. Visual Sci.* 45 (8) (2004) 2753.
- [49] J. Kezic, P.G. McMenamin, The monocyte chemokine receptor CX3CR1 does not play a significant role in the pathogenesis of experimental autoimmune uveoretinitis, *Invest. Ophthalmol. Vis. Sci.* 51 (10) (2010) 5121–5127.
- [50] C.J. Chu, P. Herrmann, L.S. Carvalho, S.E. Liyanage, J.W. Bainbridge, R.R. Ali, A.D. Dick, U.F. Luhmann, Assessment and in vivo scoring of murine experimental autoimmune uveoretinitis using optical coherence tomography, *PLoS ONE* 8 (5) (2013) e63002.
- [51] C.A. Dinarello, Overview of the IL-1 family in innate inflammation and acquired immunity, *Immunol. Rev.* 281 (1) (2018) 8–27.
- [52] J.D. Luna, C.C. Chan, N.L. Derevjanik, J. Mahlow, C. Chiu, B. Peng, T. Tobe, P.A. Campochiaro, S.A. Vinores, Blood-retinal barrier (BRB) breakdown in experimental autoimmune uveoretinitis: comparison with vascular endothelial growth factor, tumor necrosis factor alpha, and interleukin-1beta-mediated breakdown, *J. Neurosci. Res.* 49 (3) (1997) 268–280.
- [53] S.F. Abcouver, C.M. Lin, S. Shamugam, A. Muthusamy, A.J. Barber, D.A. Antonetti, Minocycline prevents retinal inflammation and vascular permeability following ischemia-reperfusion injury, *J. Neuroinflamm.* 10 (2013) 149.
- [54] G. Wang, Z. Li, S. Li, J. Ren, V. Suresh, D. Xu, W. Zang, X. Liu, W. Li, H. Wang, F. Guo, Minocycline Preserves the Integrity and Permeability of BBB by Altering the Activity of DKK1-Wnt Signaling in ICH Model, *Neuroscience* 415 (2019) 135–146.
- [55] S. Ishimoto, J. Zhang, V.K. Gullapalli, G. Pararajasegaram, N.A. Rao, Antigen-presenting cells in experimental autoimmune uveoretinitis, *Exp. Eye Res.* 67 (5) (1998) 539–548.
- [56] H.R. Chimney, P.G. McMenamin, S.J. Dando, Macrophage physiology in the eye, *Pflugers Arch.* 469 (3–4) (2017) 501–515.
- [57] A.R. Santiago, L. Bernardino, M. Agudo-Barriuso, J. Gonçalves, Microglia in Health and Disease: A Double-Edged Sword, *Mediat. Inflamm.* 2017 (2017) 1–2.
- [58] E.I. Paschalis, F. Lei, C. Zhou, X.N. Chen, V. Kapoulea, P.C. Hui, R. Dana, J. Chodosh, D.G. Vavvas, C.H. Dohelman, Microglia Regulate Neuroglia Remodeling in Various Ocular and Retinal Injuries, *J. Immunol.* 202 (2) (2019) 539–549.
- [59] E. Blacher, S. Bashirades, H. Shapiro, D. Rothschild, U. Mor, M. Dori-Bachash, C. Kleimeyer, C. Moresi, Y. Harnik, M. Zur, M. Zabari, R.B. Brik, D. Kviatkovsky, N. Zmora, Y. Cohen, N. Bar, I. Levi, N. Amar, T. Mehlman, A. Brandis, I. Biton, Y. Küperman, M. Tsory, L. Alfahel, A. Harmelin, M. Schwartz, A. Israelson, L. Arike, M.E.V. Johansson, G.C. Hansson, M. Gotkine, E. Segal, E. Elinav, Potential roles of gut microbiome and metabolites in modulating ALS in mice, *Nature* 572 (7770) (2019) 474–480.
- [60] C. Janowitz, Y.K. Nakamura, C. Metea, A. Gligor, W. Yu, L. Karstens, J.T. Rosenbaum, M. Asquith, P. Lin, Disruption of Intestinal Homeostasis and Intestinal Microbiota During Experimental Autoimmune Uveitis, *Invest. Ophthalmol. Vis. Sci.* 60 (1) (2019) 420–429.
- [61] S. Rowan, A. Taylor, The Role of Microbiota in Retinal Disease, 1074 (2018) 429–435.
- [62] R. Horai, R.R. Caspi, Microbiome and Autoimmune Uveitis, *Front. Immunol.* 10 (2019) 232.
- [63] V.R. Figliuolo, L.M. Dos Santos, A. Abalo, H. Nanini, A. Santos, N.M. Brittes, C. Bernardazzi, H.S.P. de Souza, L.Q. Vieira, R. Coutinho-Silva, C. Coutinho, Sulfate-reducing bacteria stimulate gut immune responses and contribute to inflammation in experimental colitis, *Life Sci.* 189 (2017) 29–38.
- [64] C. Cremon, S. Guglielmetti, G. Gargari, V. Taverniti, A.M. Castellazzi, C. Valsecchi, C. Tagliacarne, W. Fiore, M. Bellini, L. Bertani, D. Gambaccini, M. Cicala, B. Germana, M. Vecchi, I. Pagano, M.R. Barbaro, L. Bellacosa, V. Stanghellini, G. Barbara, Effect of Lactobacillus paracasei CNCM I-1572 on symptoms, gut microbiota, short chain fatty acids, and immune activation in patients with irritable bowel syndrome: A pilot randomized clinical trial, *United Eur. Gastroenterol.* 6 (4) (2018) 604–613.
- [65] T. Tian, B. Xu, Y. Qin, L. Fan, J. Chen, P. Zheng, X. Gong, H. Wang, M. Bai, J. Pu, J. Lu, W. Zhou, L. Zhao, D. Yang, P. Xie, Clostridium butyricum miyairi 588 has preventive effects on chronic social defeat stress-induced depressive-like behaviour and modulates microglial activation in mice, *Biochem. Biophys. Res. Commun.* 516 (2) (2019) 430–436.
- [66] T.R. Wu, C.S. Lin, C.J. Chang, T.L. Lin, J. Martel, Y.F. Ko, D.M. Ojcius, C.C. Lu, J.D. Young, H.C. Lai, Gut commensal Parabacteroides goldsteinii plays a predominant role in the anti-obesity effects of polysaccharides isolated from *Hirsutella sinensis*, *Gut* 68 (2) (2019) 248–262.
- [67] A.M. Neyrinck, U. Etxeberria, B. Tamini, G. Daube, M. Van Hul, A. Everard, P.D. Cani, L.B. Bindels, N.M. Delzenne, Rhubarb extract prevents hepatic inflammation induced by acute alcohol intake, an effect related to the modulation of the gut microbiota, *Mol. Nutr. Food Res.* 61 (1) (2017).
- [68] A.S. Arellano Buendia, M. Tostado Gonzalez, O. Sanchez Reyes, F.E. Garcia Arroyo, R. Arguello Garcia, E. Tapia, L.G. Sanchez Lozada, H. Osorio Alonso, Immunomodulatory Effects of the Nutraceutical Garlic Derivative Allicin in the Progression of Diabetic Nephropathy, *Int. J. Mol. Sci.* 19 (10) (2018).
- [69] S. Panyod, W.K. Wu, K.H. Lu, C.T. Liu, Y.L. Chu, C.T. Ho, W.W. Hsiao, Y.S. Lai, W.C. Chen, Y.E. Lin, S.H. Lin, M.S. Wu, L.Y. Sheen, Allicin Modifies the Composition and Function of the Gut Microbiota in Alcoholic Hepatic Steatosis Mice, *J. Agric. Food. Chem.* 68 (10) (2020) 3088–3098.
- [70] W. Ren, L. Zou, Z. Ruan, N. Li, Y. Wang, Y. Peng, G. Liu, Y. Yin, T. Li, Y. Hou, G. Wu, Dietary L-proline supplementation confers immunostimulatory effects on activated *Pasteurella multocida* vaccine immunized mice, *Amino Acids* 45 (3) (2013) 555–561.
- [71] B.C. Koner, B.D. Banerjee, A. Ray, Effects of in-vivo generation of oxygen free radicals on immune responsiveness in rabbits, *Immunol. Lett.* 59 (3) (1997) 127–131.
- [72] W. Lee, H. Su Kim, G.R. Lee, Leukotrienes induce the migration of Th17 cells, *Immunol. Cell Biol.* 93 (5) (2015) 472–479.
- [73] T. Liao, Y. Ke, W.H. Shao, B. Haribabu, H.J. Kaplan, D. Sun, H. Shao, Blockade of the interaction of leukotriene b4 with its receptor prevents development of autoimmune uveitis, *Invest. Ophthalmol. Vis. Sci.* 47 (4) (2006) 1543–1549.
- [74] J. Xu, X. Zhang, Q. Qian, Y. Wang, H. Dong, N. Li, Y. Qian, W. Jin, Histamine upregulates the expression of histamine receptors and increases the neuroprotective

- effect of astrocytes, *J. Neuroinflamm.* 15 (1) (2018) 41.
- [75] L. Li, L. Feng, W.D. Jiang, J. Jiang, P. Wu, S.Y. Kuang, L. Tang, W.N. Tang, Y.A. Zhang, X.Q. Zhou, Y. Liu, Dietary pantothenic acid deficiency and excess depress the growth, intestinal mucosal immune and physical functions by regulating NF-kappaB, TOR, Nrf2 and MLCK signaling pathways in grass carp (*Ctenopharyngodon idella*), *Fish Shellfish Immunol.* 45 (2) (2015) 399–413.
- [76] H. Bartolomaeus, A. Balogh, M. Yakoub, S. Homann, L. Marko, S. Hoges, D. Tsvetkov, A. Krannich, S. Wundersitz, E.G. Avery, N. Haase, K. Kraker, L. Hering, M. Maase, K. Kusche-Vihrog, M. Grandoch, J. Fielitz, S. Kempa, M. Gollasch, Z. Zhumadilov, S. Kozhakhetov, A. Kushugulova, K.U. Eckardt, R. Dechend, L.C. Rump, S.K. Forslund, D.N. Muller, J. Stegbauer, N. Wilck, Short-Chain Fatty Acid Propionate Protects From Hypertensive Cardiovascular Damage, *Circulation* 139 (11) (2019) 1407–1421.
- [77] R. Horai, C.R. Zarate-Blades, P. Dillenburg-Pilla, J. Chen, J.L. Kielczewski, P.B. Silver, Y. Jittayasothon, C.C. Chan, H. Yamane, K. Honda, R.R. Caspi, Microbiota-Dependent Activation of an Autoreactive T Cell Receptor Provokes Autoimmunity in an Immunologically Privileged Site, *Immunity* 43 (2) (2015) 343–353.
- [78] V. Brundula, N.B. Rewcastle, L.M. Metz, C.C. Bernard, V.W. Yong, Targeting leukocyte MMPs and transmigration: minocycline as a potential therapy for multiple sclerosis, *Brain: A J. Neurol.* 125 (Pt 6) (2002) 1297–1308.
- [79] J.N. Hahn, D.K. Kaushik, M.K. Mishra, J. Wang, C. Silva, V.W. Yong, Impact of Minocycline on Extracellular Matrix Metalloproteinase Inducer, a Factor Implicated in Multiple Sclerosis Immunopathogenesis, *J. Immunol.* 197 (10) (2016) 3850–3860.
- [80] Y.K. Nakamura, C. Janowitz, C. Metea, M. Asquith, L. Karstens, J.T. Rosenbaum, P. Lin, Short chain fatty acids ameliorate immune-mediated uveitis partially by altering migration of lymphocytes from the intestine, *Sci. Rep.* 7 (1) (2017) 11745.
- [81] W. Wu, Z. Zhang, T. Xiong, W. Zhao, R. Jiang, H. Chen, X. Li, Calcium ion coordinated dexamethasone supramolecular hydrogel as therapeutic alternative for control of non-infectious uveitis, *Acta Biomater.* 61 (2017) 157–168.
- [82] L. Luo, J. Yang, Y. Oh, M.J. Hartsock, S. Xia, Y.C. Kim, Z. Ding, T. Meng, C.G. Eberhart, L.M. Ensign, J.E. Thorne, W.J. Stark, E.J. Duh, Q. Xu, J. Hanes, Controlled release of corticosteroid with biodegradable nanoparticles for treating experimental autoimmune uveitis, *J. Cont. Rel. Off. J. Contr. Rel. Soc.* 296 (2019) 68–80.